Aus der

Medizinischen Universitätsklinik und Poliklinik Tübingen

Abteilung VIII, Medizinische Onkologie und Pneumologie

# Suicide gene "armed" virotherapy as a novel approach for the treatment of locally advanced or metastatic pancreatic cancer

**Inaugural-Dissertation**
**zur Erlangung des Doktorgrades**
**der Medizin**

**der Medizinischen Fakultät**
**der Eberhard Karls Universität**
**zu Tübingen**

**vorgelegt von**

**Klein, Constantin Kon-Hwa**

**2025**

| | |
|---|---|
| Dekan: | Professor Dr. B. Pichler |
| 1. Berichterstatter: | Professor Dr. U.M. Lauer |
| 2. Berichterstatter: | Professorin Dr. R. Klein |
| Tag der Disputation: | 17.06.2025 |

Meiner mich immer unterstützenden Familie Jessica, Matilda, Greta und Lilia

**TABLE OF CONTENTS**

**Abbreviations**

| | |
|---|---|
| 5-FC | 5-fluorocytosine |
| 5-FU | 5-flurorouracil |
| ADP | adenovirus death protein |
| APS | Ammonium persulfate |
| BSA | bovine serum albumin |
| CD | cytosine deaminase |
| CD | cluster of differentiation |
| CNS | central nervous system |
| CT | computed tomography |
| DAMP | damage-associated molecular pattern molecule |
| dd | double distilled |
| DMEM | Dulbecco's modified Eagle's medium |
| DMSO | Dimethyl sulfoxide |
| DNA | Deoxyribonucleic acid |
| e.g. | exempli gratia – "for example" |
| EDTA | Ethylenediaminetetraacetic acid |
| EEV | extracellular enveloped virus |
| ELISA | Enzyme-linked immunosorbent assay |
| EMA | European Medicines Agency |
| et al. | et alii – "and others" |
| F | fusion- (protein) |
| FACS | Fluorescence-activated cell sorting (Flow cytometry) |
| FBS | fetal bovine serum |
| FDA | Food and drug administration of the United States of America |
| Fig. | figure |
| g | Gravity constant of earth defined as 9.80665 $m/s^2$ |
| GFP | green fluorescent protein |
| GM-CSF | Granulocyte-macrophage colony-stimulating factor |
| H | hemagglutinin (protein) |
| HCl | hydrochloride |
| hpi | hours post infection |

| | |
|---|---|
| HSV | herpes simplex virus |
| i.e. | id est – “that means” |
| IEV | intracellular enveloped virus |
| IMV | intracellular mature virus |
| itu- | intratumoral |
| iv- | intravenous |
| kb | kilo based |
| kDa | kilo Dalton |
| L | large (protein) |
| $LD_{50}$ | median lethal dose |
| M | matrix (protein) |
| MeV | measles virus |
| MOI | multiplicity of infection |
| N | nucleocapsid (protein) |
| n/a | not available |
| NDV | Newcastle disease virus |
| OV | oncolytic virotherapy |
| P | phospho- (protein) |
| PAMP | pathogen-associated molecular pattern molecule |
| PanIN | pancreatic intraepithelial neoplasia |
| PBS | phosphate buffered saline |
| PDAC | pancreatic ductal adenocarcinoma |
| PR | partial remission |
| PVDF | polyvinylidene difluoride |
| RNA | Ribonucleic acid |
| rpm | rounds per minute |
| SCD | Super cytosine deaminase |
| SD | standard deviation |
| SD | stable disease |
| SDS-PAGE | Sodium-dodecylsulfate-polyacrylamide gel electrophoresis |
| SLAM | signaling lymphocyte-activation molecule |
| SRB | Sulforhodamine B |

| | |
|---|---|
| TAA | tumor-associated antigen |
| TBS | Tris buffered saline |
| TCA | trichloroacetic acid |
| TEMED | Tetramethylethylenediamine |
| Tris | tris(hydroxymethyl)aminomethane |
| UV | ultraviolet (wavelength between 400 nm and 10 nm) |
| VACV | vaccinia virus |
| vs. | versus |
| y.o. | years old |

# 1 Introduction

## 1.1 Pancreatic cancer (PDAC)

### 1.1.1 Epidemiological traits of PDAC

The term „Pancreatic cancer“ is usually used as a synonym for the pancreatic ductal adenocarcinoma (PDAC), which is defined as a cancer derived from the exocrine part of the pancreas. PDAC represents about 85 % of all malignant pancreatic lesions (Siegel et al., 2013). In Germany, pancreatic cancer ranks 6$^{th}$ in men and women concerning the rate of newly diagnosed cancers (non-solid tumors excluded) (*Table 1*).

**Table 1: Statistics obtained from Zentrum für Krebsregisterdaten / Robert-Koch Institut „Krebs in Deutschland 2005/2006“, „Krebs in Deutschland 2011/2012“ & „Krebs in Deutschland 2017/2018“**

| | **Incidence – Men** | | | | **Incidence – Women** | | | |
|---|---|---|---|---|---|---|---|---|
| | **Entity** | **2018** | **2012** | **2006** | **Entity** | **2018** | **2012** | **2006** |
| 1 | Prostate | 65.200 | 63.710 | 60.120 | Breast | 69.900 | 69.550 | 57.970 |
| 2 | Lung | 35.290 | 34.490 | 32.500 | Colorectal | 26.710 | 28.490 | 32.440 |
| 3 | Colorectal | 33.920 | 33.740 | 36.300 | Lung | 21.930 | 18.030 | 14.600 |
| 4 | Bladder | 13.500 | 11.270 | 19.360 | Melanoma | 10.880 | 10.930 | 11.140 |
| 5 | Melanoma | 12.010 | 10.400 | 7.360 | Uterus | 10.860 | 10.420 | 8.470 |
| **6** | **Pancreas** | **9.860** | **8.250** | **6.380** | **Pancreas** | **9.160** | **8.480** | **6.980** |
| 7 | Mouth / Pharynx | 9.820 | 9.290 | 7.930 | Ovarian | 7.300 | 7.380 | 9.670 |
| 8 | Kidney | 9.350 | 9.500 | 10.050 | Gastric | 5.560 | 6.460 | 7.230 |
| 9 | Gastric | 9.200 | 9.180 | 10.620 | Kidney | 5.480 | 5.530 | 6.440 |
| 10 | Liver | 6.690 | 6.020 | n/a | Bladder | 4.770 | 4.140 | 8.090 |

Even more impressive than the incidence rate, is the high mortality rate. Statistically, pancreatic cancer ranks 4$^{th}$ in both men and women in terms of cancer related death (*Table 2*). This is due to the very poor prognosis of

pancreatic cancer, leading to the conclusion, that almost all patients diagnosed with pancreatic cancer will eventually have a fatal course.

**Table 2: Statistics obtained from Robert-Koch Institut „Krebs in Deutschland 2005/2006“, „Krebs in Deutschland 2011/2012“ & „Krebs in Deutschland 2017/2018“.**

| | **Mortality – Men** | | | | **Mortality – Women** | | | |
|---|---|---|---|---|---|---|---|---|
| | **Entity** | **2018** | **2012** | **2006** | **Entity** | **2018** | **2012** | **2006** |
| 1 | Lung | 28.365 | 29.713 | 28.898 | Breast | 18.591 | 17.748 | 17.286 |
| 2 | Prostate | 14.963 | 12.957 | 11.577 | Lung | 16.514 | 14.752 | 11.873 |
| 3 | Colorectal | 13.240 | 13.772 | 13.756 | Colorectal | 11.008 | 12.200 | 13.469 |
| **4** | **Pancreas** | **9.189** | **7.936** | **6.729** | **Pancreas** | **9.143** | **8.184** | **7.213** |
| 5 | Liver | 5.301 | 5.117 | n/a | Ovarian | 5.326 | 5.646 | 5.636 |
| 6 | Gastric | 5.187 | 5.770 | 5.986 | Gastric | 3.674 | 4.208 | 4.937 |
| 7 | Esophagus | 4.278 | 4.072 | 3.642 | Liver | 2.689 | 2.553 | n/a |
| 8 | Mouth / Pharynx | 3.970 | 4.090 | 3.623 | Uterus | 2.631 | 2.515 | 2.395 |
| 9 | Bladder | 3.862 | 3.791 | 3.549 | CNS | 2.615 | 2.591 | 2.600 |
| 10 | CNS | 3.441 | 3.293 | 2.955 | Biliary tract | 2.017 | 2.122 | n/a |

CNS: central nervous system

Although, management and detection rates have improved significantly over the last years for many tumor entities, the prognosis for pancreatic cancer remains dismal. 5 years after diagnose, only ~4 % of patients are still alive. Mainly this poor prognosis is due to the absence of early symptoms or reliable / effective screening methods. Patients with pancreatic cancer mostly present with unspecific symptoms, like weight loss, fatigue and abdominal pain or with the more specific painless jaundice. This leads to the devastating fact that in only 15 - 20 % of all cases, pancreatic cancer is diagnosed in a curative, resectable stage

(stage I/II), as 35 % present in with locally advanced (stage III) or metastatic disease (stage IV) (Stathis et al., 2010) (Vincent et al., 2011).

### 1.1.2 Pathogenesis and characteristics of PDAC:

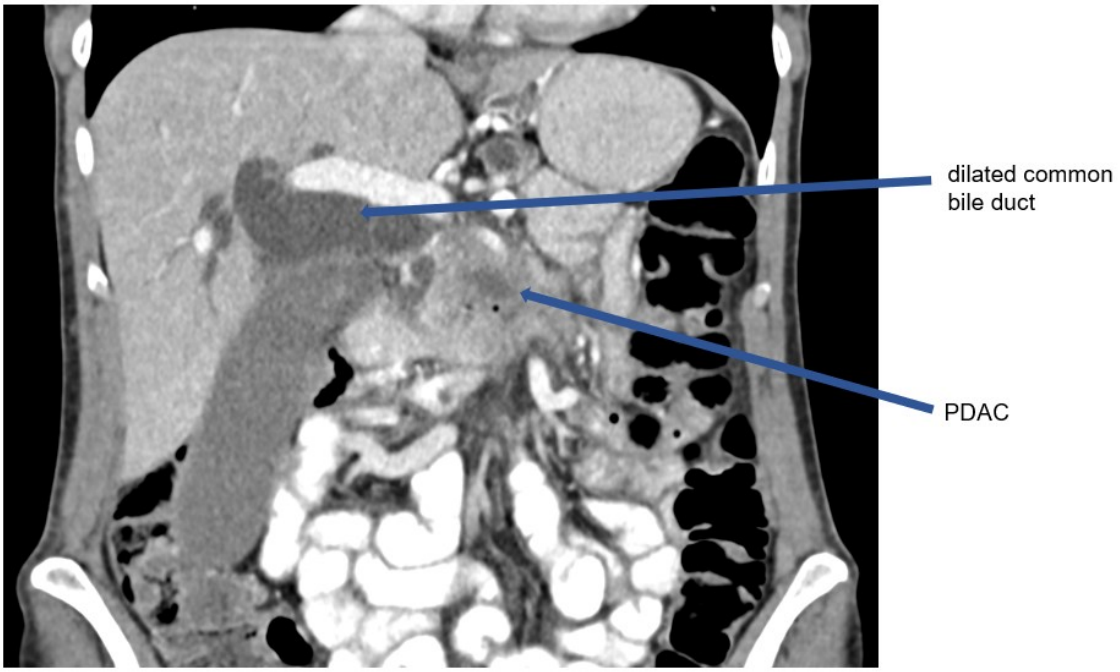


**Fig. 1: Contrast enhanced CT scan image from a patient suffering from of a locally advanced PDAC in the pancreas head, causing intra- and extrahepatic cholestasis due to obstruction of the common bile duct.**

The pancreas is an organ which belongs to the digestive and endocrine system of the human body. PDAC arises from the exocrine part of the pancreas, which is mainly located in the pancreas head (*Fig. 1*). In a database research study with information from 100.313 patients from the United States, PDAC developed in 78 % in the head, 11 % in the body and also 11 % in the tail (Sener et al., 1999).
On a cellular level, PDAC originates from the ductal epithelium of the exocrine pancreas, initially forming asymptomatic premalignant lesions (Hidalgo M, 2010). There are several different kinds of facultative precursors for PDAC, like the intraepithelial neoplasia (PanIN), the intraductal papillary mucinous neoplasm (IPMN), the intraductal tubulopapillary neoplasm (ITPN), the intraductal oncocytic papillary neoplasm (IOPN) and the mucinous cystic neoplasm (MCN) (Kim et al., 2018). Although the PanIN is the one precursor which cannot be detected by current imaging techniques, the histologic transition from low-grade-dysplasia to

high-grade-dysplasia to malignant transformation is well known and understood (*Fig. 2*).

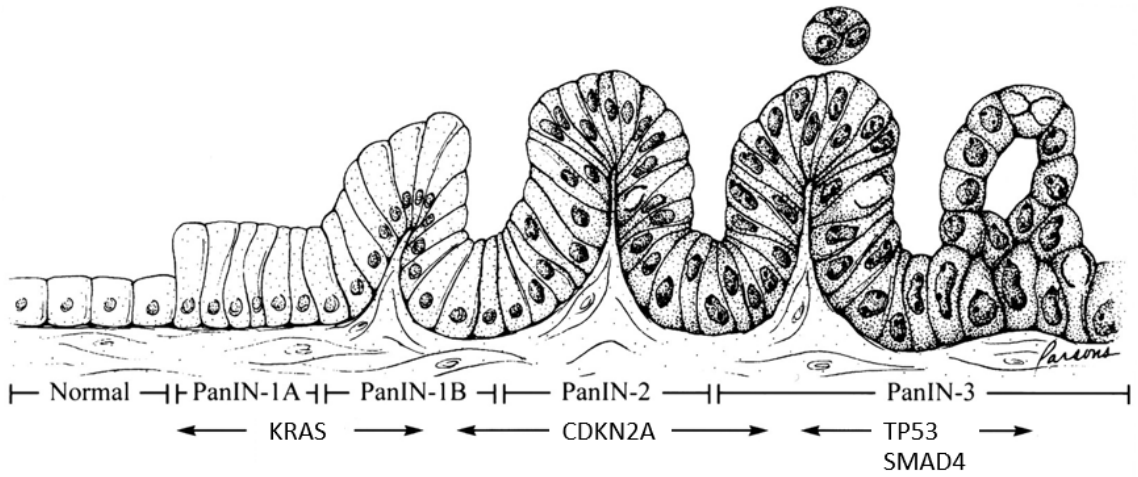


**Fig. 2: Schematic representation of a histologically defined PDAC progression model.** Malignant transformation is depicted left to right with progression of normal tissue to PanIN (pancreatic intraepithelial neoplasia) lesions. The bottom row displays typical genetic alterations, like *KRAS* (Kirsten rat sarcoma viral oncogene), *CDKN2A* (Cyclin Dependent Kinase Inhibitor 2A), *TP53* and *SMAD4* (SMAD Family Member 4), which are often acquired during carcinogenesis. This figure was obtained and modified from Hruban et al., 2000.

On a molecular level the formation and progression of PDAC precursor lesions is the result of accumulation of different genetic alterations (Vogelstein et al., 2004). The mutational landscape of 100 different PDACs has recently been investigated by whole genome sequencing and copy number analysis, suggesting to classify PDAC into the 4 different subtypes “stable”, “locally rearranged”, “scattered” and “unstable”, which are to date not clinically established (Waddel et al., 2015). The typically found mutations in PDAC are:

- Aberrant activation of the oncogene *KRAS*, resulting in an activation of the MAPK/ERK pathway, which propagates cellular growth (Downward J, 2003)
- Inactivation of tumor-suppressor gene *CDKN2A* (cyclin-dependent kinase inhibitor 2A), which encodes for the proteins p16 and p14ARF. Especially p16 plays a crucial role in cell cycle regulation, as it can normally induce cell cycle arrest upon detected DNA-damage (Liggett Jr WH, 1998).
- Inactivation of *TP53*, encoding for p53, which is often referred to as “the guardian of the genome”. Fully functioning, it is able to eliminate cells which

have acquired DNA-damage and limits oncogene-expressing aberrant cells to proliferate (Kastenhuber et al., 2017)

- Inactivation of the *SMAD4* gene, encoding for the similar named protein SMAD4. It works as a transcription factor, mediating the transduction of the growth factor TGF-β. Upon mutation, TGF-β accumulates, promoting proliferation and therefore tumor growth (Xia et al., 2015).

Once malignant transformation has occurred, PDAC typically features certain traits. Common histopathologic features are a high content of desmoplasia and stromal surroundings. Myofibroblasts, mixed with extracellular matrix material, like type I collagen and hyaluronic acid, together with inflammatory cells, like macrophages, lymphocytes and mast cells form a tumor-microenvironment that plays an important role in tumor growth and sustainment. PDACs are typically characterized as hypovascular, resulting in a reduced blood supply (Ryan et al., 2014).

### 1.1.3 Treatment of PDAC

To date, early resection of the tumor in a localized stage is the only curable treatment for pancreatic cancer. Is resection not a feasible option (locally advanced or metastatic disease), palliative chemotherapy is the treatment of choice (Ryan et al., 2014). Before 1997, the standard treatment regimen was a 5-fluoruracil mono therapy, until a mono therapy with gemcitabine replaced this therapy because of improvement of survival and clinical benefits, in terms of treatment related side effects (Burris et al., 1997). Both compounds are still used for the treatment of locally advanced or metastatic disease, but nowadays these substances are components of more aggressive combined chemotherapy regimens.

The first line treatment for patients in a generally acceptable health state is a combination therapy, consisting of 5-fluoruracil, folinic acid, oxaliplatin and irinotecan, called FOLFIRINOX. This aggressive chemotherapy regime is to date the most effective treatment option (in terms of overall survival). In a large (n = 342), randomized clinical trial, it could improve overall survival from 6.8 months to 11.1 months with a response rate of 31 % (for FOLFIRINOX) vs. 9 %. A state-

of-the-art gemcitabine-monotherapy served as control (Conroy et al., 2011). Survival benefit is achieved at the cost of a significantly higher toxicity of the FOLFIRINOX regimen (e.g. nausea / vomiting, myelosuppression, diarrhea). Current studies in the adjuvant / neoadjuvant setting (Conroy et al., 2018) tend to use a modified FOLFIRINOX protocol with reduction of the 5-fluorouracil dose in order to limit toxicity and increase therapy adherence (Mahaseth et al., 2013). Also, a combination therapy with gemcitabine and nab-paclitaxel is used as a first-line therapy as it improves survival compared with a gemcitabine-monotherapy from 6.7 months to 8.5 months (Von Hoff et al., 2013).

One could state that there are valid treatment options available, but the prognosis of pancreatic cancer remains extremely poor. Despite all efforts, the standard treatment prolongs survival statistically for only a few months. Also, often treatment is hampered by commonly seen therapy associated toxicity. Therefore, new, effective and well tolerated treatment approaches are desperately needed.

## 1.2 Oncolytic virotherapy

### 1.2.1 Principles of oncolytic virotherapy

In the early 1970s, first reports of spontaneous regression of non-solid tumors after a wild-type measles virus infection laid the foundation of today's virotherapeutic concepts (Bluming et al., 1971). The term "oncolytic virotherapy" (OV) describes the approach to use replication competent viruses as therapeutic agents for cancer treatment. Ideally, an oncolytic virus selectively targets cancer cells while sparing healthy tissue, resulting in an antitumor effect with less systemic side effects than standard chemotherapy (*Fig. 3*). Once the virus has entered the cancer cell, it takes over its protein synthesis and begins to produce progeny virus particles. This will eventually lead to lysis of the infected host cell, releasing numerous endogenous viral particles, each of them being able to infect more hitherto uninfected cancer cells.

Another mechanism of the oncolytic effect would be the activation of the host immune system. Virus-mediated apoptosis / necrosis can lead to the release of cytokines, damage-associated molecular pattern molecules (DAMPs), tumor-associated antigens (TAAs) and pathogen-associated molecular pattern

molecules (PAMPs) which can be taken up by antigen-presenting cells of the host cellular immune system. By presenting these immunogenic fragments to $CD4^+$ and $CD8^+$ T cells, this can lead to activation of the adaptive immune system, resulting in an anti-tumoral immune response distant to the initially infected tumor-site (Lemos de Matos et al., 2020).

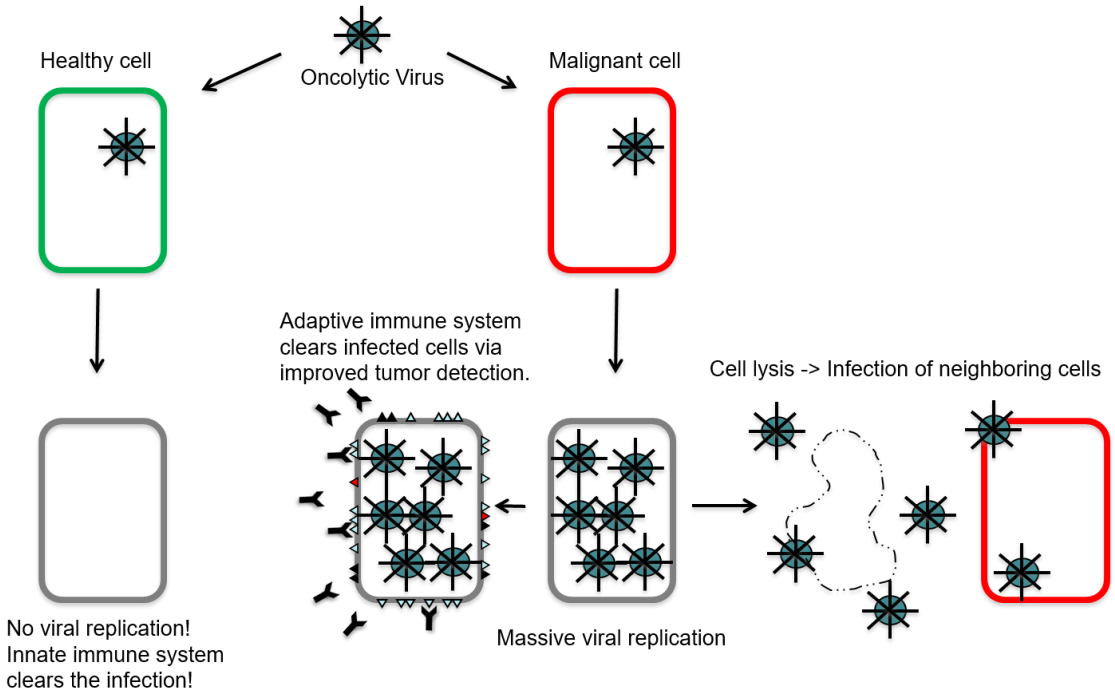


**Fig. 3: Principles of oncolytic virotherapy.** Most oncolytic viruses are to a certain degree attenuated but able to infect both healthy and malignant cells. Whereas in healthy cells the infection with the attenuated viruses can easily be cleared by activating the innate immune system and/or by going into apoptosis, malignant cells have obtained many mutations, often in pathways related to innate immunity or apoptosis. Therefore, infected malignant cells are unable to clear the infection and the oncolytic virus is able to replicate solely within the cancer cells. This will eventually lead to infection related lysis of the cell, enabling the released viral particles to infect neighboring cancer cells as well. Another aspect of antitumor effect is that the inflammation may trigger the adaptive immune system, as cell lysis releases DAMPs, PAMPs and TAAs into extracellular space and therefore leads to an improved tumor detection.

*Fig. 3* shows the course of action of how an oncolytic virus ideally works. There are several different viruses, e.g. herpes simplex virus, reovirus, adenovirus, coxsackie virus, Newcastle disease virus, parvovirus, poliovirus, measles vaccine virus (MeV) and vaccinia virus (VACV), which have been used in pre-/clinical

studies for OV (Lawler et al, 2017). In modern virotherapy, there are several approaches, using genetically modified, replication competent viruses to specifically target and eliminate cancer cells. By modifying the viral entry receptor, the selectivity for cancer cells and therefore the efficacy of the viral agent can be drastically increased. Also, by inserting genes into the viral genome, the oncolytic effect can be enhanced: approaches aim to increase the immune response to the infection or to enhance the virus-mediated oncolysis (Lawler et al., 2017) (Lauer et Beil, 2022). Talimogen laherparepvec (T-VEC), a herpes simplex virus type-1, was the first oncolytic virotherapeutic agent approved by the FDA- and EMA in 2015 for the treatment of non-resectable or metastatic malignant melanoma (Andtbacka et al., 2019). First preclinical trials using an oncolytic measles vaccine virus for the treatment of pancreatic cancer with promising results have been published (Bossow et al., 2011), but a clinically approved oncolytic viral agent for gastrointestinal tumor treatment is still missing.

### 1.2.2 The super cytosine deaminase suicide gene system

The term “suicide gene” describes a gene, which upon transcription leads to the expression of a protein which eventually leads to self-destruction of the host cell. The super cytosine deaminase (*SCD*) suicide gene, which can be inserted into the viral genome of an oncolytic virus, encodes for a prodrug-converting enzyme, enabling only infected tumor cells to metabolize the applied prodrug (Graepler et al., 2005).

Yeast-derived *SCD* catalyzes the deamination of the non-toxic prodrug 5-fluorocytosine (5-FC) into the well-known chemotherapeutic compound 5-fluorouracil (5-FU). The mechanism of *SCD* is depicted in *Fig. 4*.

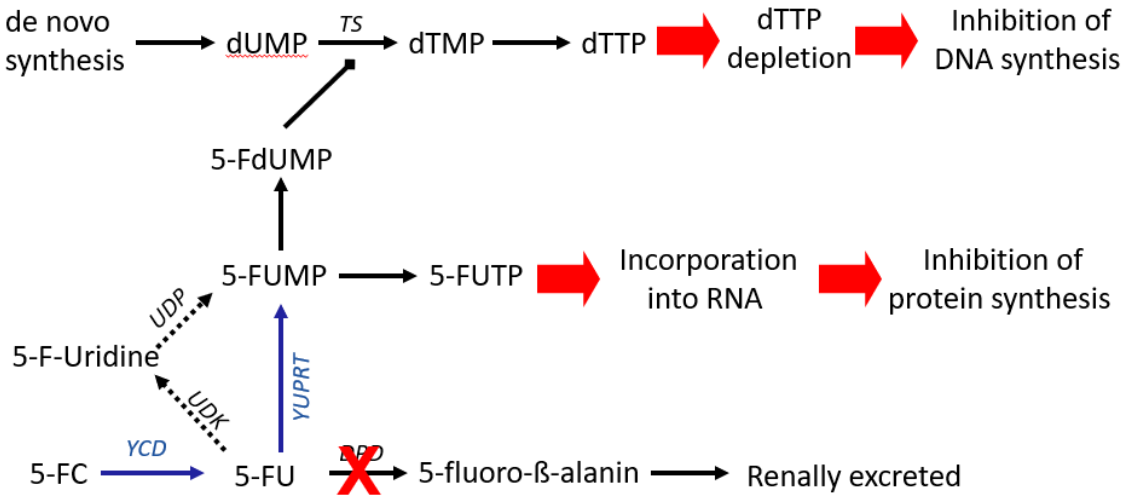


**Fig. 4: Mechanism of prodrug converting enzyme encoded by *SCD*.** *SCD* encodes for a fusion protein consisting of yeast cytosine deaminase (YCD) and yeast uracil phospho-ribosyl-transferase (YUPRT). The YCD converts the prodrug 5-FC into 5-FU, whereas the YUPRT catalyzes the metabolic conversion of 5-FU into its cytotoxic metabolite 5-FUMP. This prevents 5-FU from getting detoxified by the DPD, resulting in higher 5-FUMP levels and therefore higher toxicity (Berchtold et al., 2020). dUMP: deoxyuridine monophosphate; TS: thymidylate synthase; dTMP: deoxythymidine mono-phosphate; dTTP: deoxythymidine triphosphate; 5-FdUMP: 5-fluorodeoxyuridinemono-phosphate; 5-FUMP: 5-fluorouridinemonophosphate; 5-FUTP: 5-fluorouridine triphosphate;5-FC: 5-fluorocytosine; YCD: yeast cytosine deaminase; 5-FU: 5-fluorouracil; UDK: uridine kinase; UDP: uridine phosphorylase; YUPRT: yeast uracil phosphoribosyltransferase; DPD: dihydro-pyrimidinedehydrogenase.

By systemic application of 5-FC, only virus-infected cells harboring the *SCD* gene are able to convert the prodrug into 5-FU intracellularly, eventually resulting in apoptosis / necrosis of the infected host cell. As 5-FU is diffusible, the chemotherapeutic compound can also harm neighboring, non-infected cells in terms of a locally active bystander effect.

### 1.2.3 Oncolytic measles vaccine virus (MeV)

The measles virus (MeV) belongs to the family of *Paramyxoviridae* genus *Morbillivirus.* It is an enveloped, negative-strand RNA-Virus which encodes for six structural proteins (*Fig. 5*): The surface-bound H and F proteins are responsible for cell-entry via receptor-binding (H) and membrane fusion (F). The N, L and P proteins form a ribonucleoprotein complex with the genomic RNA and play a role in replication initiation. The M protein forms an inner layer beneath the envelope and plays a role in virus budding and transcription regulation (Yanagi et al., 2006).

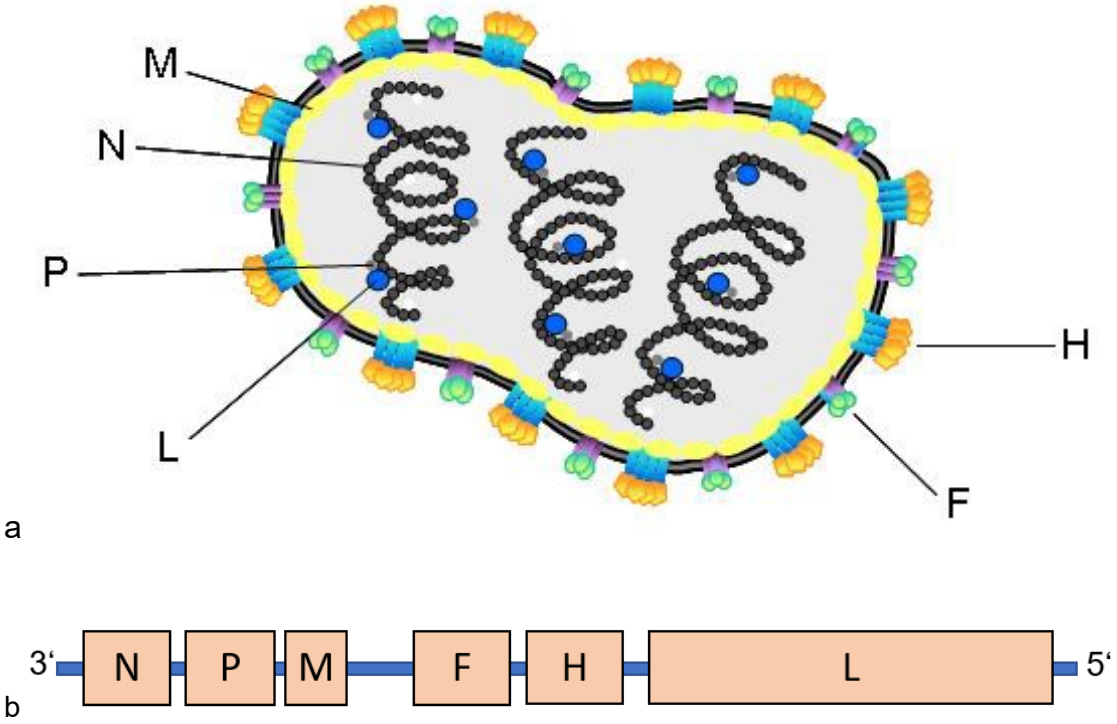


**Fig. 5: Schematic structure of MeV.**
(a) Measles virus includes six structural proteins and the negative strand RNA. N (nucleocapsid protein), P (phosphoprotein associated with RNP in polymerase complex), M (matrix protein), F (fusion glycoprotein), H (haemagglutinin), L (large protein); figure is copyrighted by *Guy Ungerechts*, NCT Heidelberg.
(b) Schematic representation of wild type MeV linear, negative strand RNA-genome. Transcription begins at the 3’ terminal, resulting in a transcription gradient with highest protein expression for genes located near the 3’ terminal and decreasing expression of gene loci further downstream.

The transcription of these proteins follows a specific gradient, starting with the most upstream located gene. This means, the amount of transcribed and expressed viral protein is strongly dependent on the location of the gene on the RNA-strand. The order, starting with the most upstream located N-Protein, followed by the P-Protein and so on, is depicted in *Fig. 5b*.

The wild type MeV interacts via the surface H- and F-proteins with the two different host cell receptors SLAM/CD150 and Nectin-4/PVRL 4 (Mühlebach et

al., 2011). It replicates solely in the cytoplasm and is not able to integrate its genome into the host's DNA-genome, as it doesn't penetrate the nucleus and lacks a reverse transcriptase. Wild type MeV causes the infectious disease "measles", which presents with typical symptoms, including a characteristic rash, fever and a dry cough. MeV's only natural host is the human (Laksono et al., 2016). Measles is accounted as one of the most contagious infectious diseases there is. It is transmitted as droplet infection and therefore spreads via the respiratory route (Moss, 2017). Once it has entered a susceptible host, it infects entry-receptor expressing myeloid, lymphoid and/or dendritic cells. Replication mainly takes place in $SLAM^{+}$-enriched lymphoid tissues, e.g. the bone marrow, spleen or lymph nodes. Upon infection, MeV spreads from cell to cell by formation of syncytia, a fusion of multiple infected cells into multinucleated giant cells (Ludlow et al., 2015). This often results in a transient immune suppression of the host, making opportunistic bacterial infections more likely to occur. The lethality of measles is estimated between 0.01 and 0.1 % in industrialized countries. Only roughly 60 % of German adults have received the recommended two consecutive measles vaccination shots and have thereby been immunized sufficiently against this disease (Kassenärztliche Bundesvereinigung, 2021).

The virus used in this study is a measles vaccine virus, Edmonston strain, which was originally isolated in 1954 from an eleven-year-old boy with the name Edmonston. The Edmonston strain was attenuated in several passages by cell culture (Combredet et al., 2003). It has lost its affinity to SLAM and Nectin-4 and uses a different host cell receptor than the wild type virus, namely the membrane cofactor protein CD46 (Dörig et al., 1993). The cluster differentiation marker CD46 is a widely distributed cell surface protein which plays an important role in the regulation of the complement system. It functions as a membrane-bound inhibitor of complement activation on host cells (Liszewski et al., 1991). CD46 serves as a promising entry-receptor for OV as it is highly expressed on a variety of malignant cells of different origin (Geller et al., 2019).

Recapitulating the characteristics of measles vaccine virus:

- being an RNA-virus, not able to insert viral genome into its host genome
- being very efficient in spreading through its target cells by forming syncytia
- has been used millions of times in humans for measles vaccinations and thus has a long record safety-profile for healthy individuals
- using CD46 as entry-receptor, which is typically overexpressed on malignant tissue

Taken together, this makes measles vaccine virus a promising candidate for oncolytic virotherapy.

### 1.2.4 Oncolytic vaccinia virus (VACV)

The vaccinia virus (VACV), member of the *Orthopoxvirus*, genus of the P*oxviridae*, is a large, brick-shaped or ovoid, enveloped ds-DNA virus of 189 kb (*Fig. 6*).

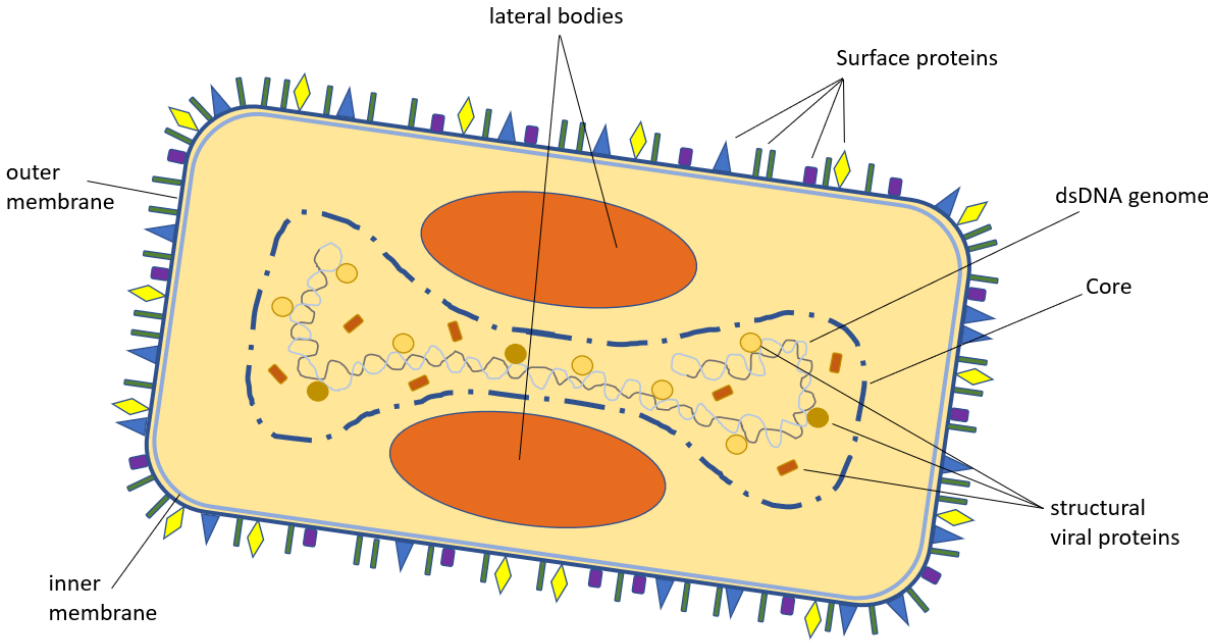


**Fig. 6: Schematic structure of a mature virion of VACV.** There are two structurally distinct forms of VACV: the intracellular mature virus (IMV) and the extracellular enveloped virus (EEV), which is depicted above. The EEV is enveloped by a dual lipid-membrane layer. The outer layer contains different surface proteins which are needed for attachment. The nucleus is biconcave shaped, flanked by the lateral bodies which function as “delivery containers” for viral enzymes. The dsDNA is embedded by regulatory / structural proteins, keeping the DNA in its densely compacted, supercoiled structure.

The origin of the vaccinia virus remains somewhat unclear to date, as the viral genome differs from the other known poxviruses like smallpox or cowpox (Baxby et al., 1977). It is common belief that it was originally derived from the cowpox virus and gained DNA alterations by repeated cultivations and passages (Antoine et al., 1998). In 1796 Edward Jenner introduced the concept of vaccination by using the vaccinia virus to prevent people from obtaining smallpox. The World Health Organisation started a campaign in 1958 to vaccinate the world's population with VACV in order to eradicate smallpox. This was achieved in 1979 when smallpox was declared eradicated worldwide. In this study, the *Lister* strain was used. This strain, which was originally derived from a Prussian soldier, was the main smallpox vaccine used in England throughout the eradication campaigns (Wilkinson et al., 1982).

The vaccinia virus does not have a known natural host, but since 1999 outbreaks have been documented in rural areas of brazil, where farm animals and farm workers got affected (Oliveira et al., 2017). Upon infection, humans can develop skin lesions, mainly on the hands, which appear as inflamed, itchy nodular swellings. Two weeks from the appearance of the skin lesions, they typically turn into necrotic ulcers, while patients can develop flu-like symptoms in terms of fever, headache and myalgia (Geessien Kroon et al., 2016).

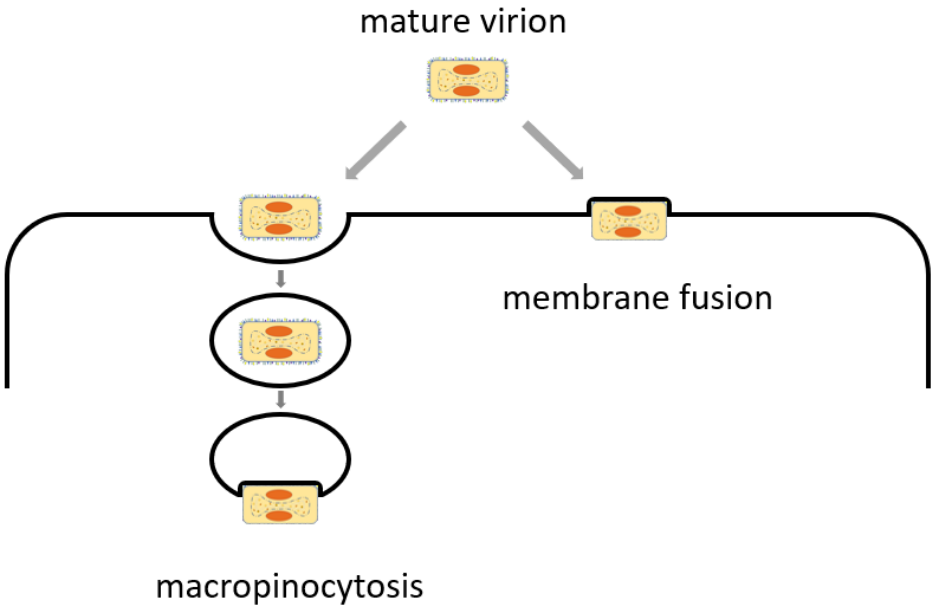

**Fig. 7: VACV cell entry.** The outer layer surface proteins bind to the host cell's surface. Via macropinocytosis, the virus (mostly the IEV form) gets taken up by a vesicle. In a second step, the viral DNA and proteins get deployed (without the dual layer membrane) into the cytoplasm. Via membrane fusion, the virus (mostly the EEV form) outer membrane, containing the surface proteins gets shed and the inner membrane fuses with the host cell's surface, releasing the core directly into the cytoplasm.

VACV does not use a specific entry-receptor: It has different techniques of cell entry, depending on the viral form (IMV vs EEV) (*Fig. 7*). The EEV enters the cell via macropinocytosis, a form of vesicle-mediated endocytosis and therefore becomes uncoated in the host cell cytoplasm (Moss B, 2021), (Mercer et al., 2009), whereas the IMV can use direct plasma membrane fusion (Schmidt et al., 2011).

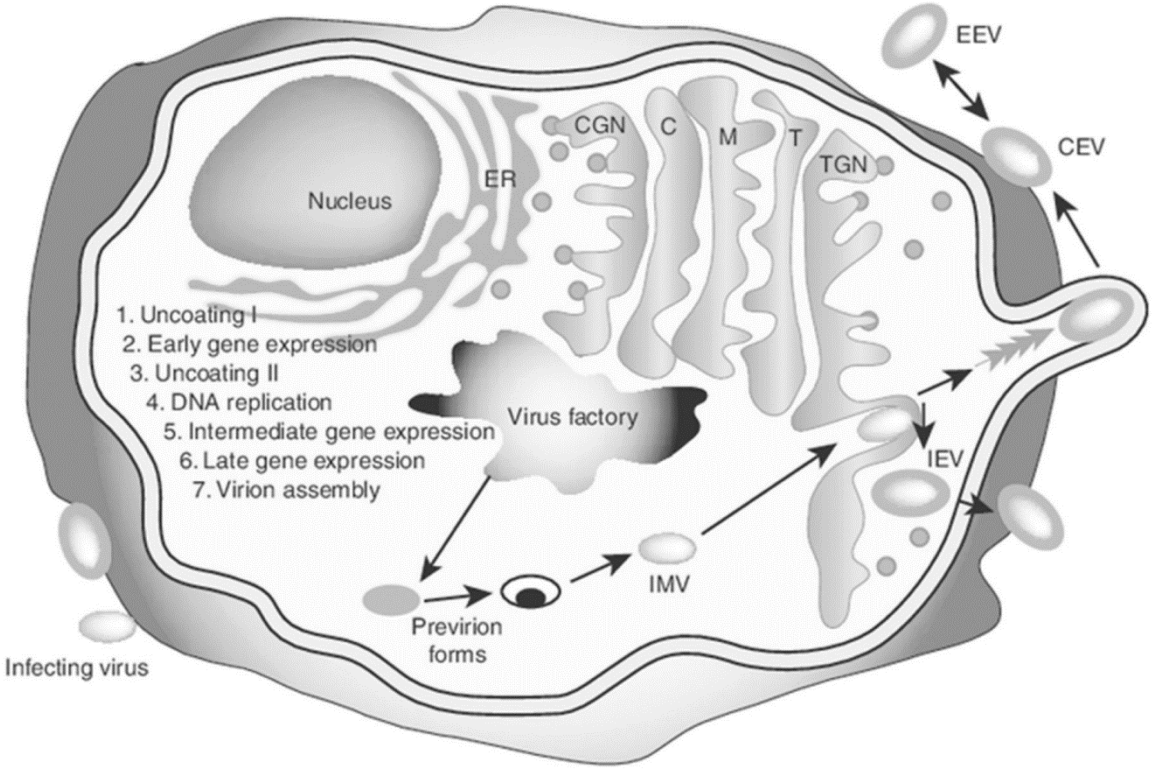


**Fig. 8: Schematic representation of VACV replication cycle** (Guo et al., 2019). ER (endoplasmic reticulum), CGN (cis-Golgi network), C (cis-Golgi), M (medial-Golgi), T (trans-Golgi), TGN (trans-Golgi network). CEV: cell-associated enveloped virus; EEV: extracellular enveloped virus; IEV: intracellular enveloped virus; IMV: intracellular mature virus.

VACV is independent of the cell nucleus, as it replicates solely in the cytoplasm (*Fig. 8*). All protein components necessary for replication are encoded in the viral

DNA. Replication follows a distinct order with sequential transcription of gene-groups, classifies as early, intermediate and late gene-groups (Broyles SS, 2003). Upon cell entry and removal of the outer viral envelope, the viral core is transferred by microtubule-transport deeper into the cytoplasm into the perinuclear region of the infected host cell (Carter et al., 2003). The replication exclusively takes place at specific “virus factories”, associated with the endoplasmatic reticulum (Tolonen et al., 2001). It is initiated by transcription of the early-gene group, which encodes for proteins that serve the replication of the viral DNA and manipulate the host cell metabolism in favor of VACV replication. The intermediate-gene group mainly encodes for regulatory viral proteins. The late-gene group encodes for structural proteins which, combined with the replicated DNA, forms new viral particles, which are able to infect neighboring cells. Around 6 hours post infection (hpi) the first viral particles are released from the host cell. At 12 hpi, already up to 10.000 copies of the viral genome have been produced and distributed (Salzman NP, 1960).

Vaccinia virus clearly is a suitable candidate for oncolytic virotherapy for several reasons:

- VACV uses a very efficient replication cycle, producing infectious particles roughly around 6 hours post infection.
- As VACV solely replicates in the cytoplasm without penetrating the nucleus of host cells, integration of viral DNA into the host genome is very unlikely.
- Vaccinia virus has already been used millions of times as a vaccination against smallpox. Its safety profile is therefore very well-known. To date, there is no known case of an airborne transmission of a vaccinia virus infection.
- The VACV DNA genome with 189 kb is fairly large for a virus and genetically very stable. This makes the virus highly versatile as it is possible to insert more than 25 kb of transgenes into the viral genome (Chen et al., 2009).

### 1.2.5 Clinical trials with oncolytic virotherapy for the treatment of pancreatic cancer

As PDAC is in dire need of a valid treatment option, pancreatic cancer is more and more becoming a target for oncolytic virotherapy studies. First reviews of completed clinical OV studies for the treatment of PDAC have been published (Haller et al., 2020). Despite the fact, that preclinical examinations with oncolytic viruses have been started in the early 1990s, there are still only few clinical trials concerning the specific treatment of pancreatic cancer (none of them being measles or vaccinia virus mediated). A complete list of all studies evaluating OV for the treatment of pancreatic cancer is depicted in Table 3).

**Table 3: Chronologic summary of all clinical trials for oncolytic virotherapy for the treatment of pancreatic cancer based on a *Pubmed.com* and *ClinicalTrials.gov* inquiry.** Trials also including other tumor entities and studies without intentional treatment (e.g. imaging studies) were excluded.

| Virus | Start | Modified | Study design | Results |
|---|---|---|---|---|
| Adenovirus (ONYX-015) | n/a | Targeted to p53 depleted cells | N=22, phase I; i.t.-injection (Mulvihill et al., 2001) | No objective responses |
| Adenovirus (ONYX-015) | 1998 | Targeted to p53 depleted cells | N=21; phase I/II; i.t.-injection, combined with gemcitabine (Hecht et al., 2003) | 2x PR, 6x SD |
| HSV-1 (HF-10) | 2005 | attenuated | N=6, phase I; intraoperative i.t.-injection (if not primarily resectable) + biopsy (Nakao et al, 2011) | 1x PR, 3x SD |
| HSV-1 (T-VEC) | 2006 | Attenuated; encoding for GM-CSF for enhanced immune response | N=17, phase I/II; i.t.-injection with 3 doses, each 3 weeks apart (ClinicalTrials.gov, NCT00402025) | no objective response |
| Reovirus (Reolysin) | 2009 | none | N=34, phase II; repeated i.v.-infusions + gemcitabine (Mahalingam et al., 2018) | 1xPR, 23x SD |
| Reovirus (Reolysin) | 2010 | none | N=73, phase II (randomized); repeated i.v.-infusion + Carboplatin / Paclitaxel vs Carboplatin / Paclitaxel (Noonan et al., 2016) | No significant benefit vs. control |
| Adenovirus (VCN-01) | 2014 | Targeted to pRB deregulated cells; encoding for hyaluronidase to enhance tissue penetration | N=8, phase I; i.t.-injection, combined with gemcitabine + nab-paclitaxel (ClinicalTrials.gov, NCT02045589) | Closed; results pending |
| Parvovirus H-1 (ParvOryx) | 2015 | None | N=7, phase II; Repeated i.v.-infusions and i.t.-injection (Hajda et al., 2017) | 2x PR |
| Reovirus (Reolysin) | 2015 | none | N=11, phase Ib; repeated i.v.-infusion + pembrolizumab + chemotherapy (5-FU or gemcitabine or irinotecan) (Malalingam et al., 2020) | 1x PR, 2x SD |
| Adenovirus (Theragene®) | 2016 | Encoding for cytosine deaminase / ADP to enhance oncolysis | N=9, phase I; i.t.-injection + 5-FC + valganciclovir + gemcitabine (Lee et al., 2020) | 1x PR, 8x SD |

| | | | | |
|---|---|---|---|---|
| Adenovirus (LOAd703) | 2016 | Encoding for CD40L and 4-1BBL as immune-activators | N=43; phase I/II; i.t.-injection, combined with gemcitabine (ClinicalTrials.gov, NCT02705196) | still recruiting |
| HSV-1 (HF10) | 2017 | attenuated | N=36, phase I (randomized); repeated i.t.-injections + either gemcitabine / nab-paclitaxel or TS-1 (ClinicalTrials.gov, NCT03252808) | Closed, results pending |
| Reovirus (Reolysin) | 2018 | None | N=12, phase II; Repeated i.v.-infusions + pembrolizumab (ClinicalTrials.gov, NCT03723915) | 1x PR |
| HSV-2 (OH2) | 2021 | Encoding for GM-CSF for enhanced immune response | N=25, phase Ib/II; repeated i.t.-injections (ClinicalTrials.gov, NCT04637698) | still recruiting |
| Adenovirus (H101) | 2022 | E1B-deletion for enhanced replication | N=25, phase Ib; i.t.-injection + Tislezizumab / Lenvatinib (ClinicalTrials.gov, NCT05303090) | Still recruiting |

ADP: adenovirus death protein

HSV: herpes simplex virus

i.t.-: intratumoral

i.v.: intravenous

PR: partial remission

SD: stable disease

Most of the already performed clinical trials were phase I or phase I/II studies with only few patients treated. Also, only 2 of the above listed studies were randomized, making it difficult to abstract the actual significance of OV.

In 2020 the results of a randomized clinical trial using a wild type reovirus (REOLYSIN®) was published. 73 patients received either REOLYSIN® as an i.v. infusion in combination with the chemotherapeutic compounds carboplatin and paclitaxel, whereas the control group was treated solely with carboplatin and paclitaxel. Unfortunately, the study didn't show any significant benefit for the virotherapy-combined treatment over standard chemotherapy treatment (Noonan et al., 2016).

The only other randomized study, uses an attenuated HSV-1 (HF10) which is directly administered intratumorally via endoscopic-ultrasound guided injection. Randomization is either the OV treatment in combination with chemotherapeutic

compounds gemcitabine and nab-paclitaxel vs. in combination with a different chemotherapy (TS-1, a prodrug of 5-FU). 36 patients were included. Despite the concept of this study surely looks interesting, the benefit from OV treatment will be difficult to determine, as all patient receive the OV treatment. Although the study is already closed, results are yet unpublished (ClinicalTrials.gov, NCT03252808).

A noteworthy human trial without direct treatment of the patient was done in 2007 with the genetically modified oncolytic virus “NV1066”, HSV-1 derived and encoding for GFP. In this study, 82 patients with PDAC, suffering from ascites (undiagnosed but most likely due to peritoneal metastasis) were enrolled. Ascites was obtained, infected with NV1066, examined regularly via cytology and via fluorescence microscopy (as infected tumor cells should express GFP). The fluorescence enhanced microscopy after incubation with NV1066 had increased the positive results by 46 % (Kelly et al., 2016).

Considering the data that can be obtained from already published clinical studies, the question, if oncolytic virotherapy is a valid option for the treatment of pancreatic cancer, cannot be answered sufficiently yet.

### 1.3 Objectives:

The aim of this dissertation was to evaluate, whether two prototypic suicide gene-encoding virotherapeutic vectors (i.e., the measles vaccine virus-based MeV-SCD and the vaccinia virus-based GLV-1h94) could suit as highly effective therapeutic agents for the treatment of pancreatic cancer.

Thus, this dissertation first sought to gather preclinical data to prove the principle of suicide-gene armed virotherapy in pancreatic cancer in order to overcome the well-known resistances to conventional chemotherapeutic regimens.

As a secondary aim it was investigated whether the usage of two different types of suicide gene-encoding viruses (MeV-SCD and GLV-1h94) would provide different outcome patterns concerning their features of resistance or susceptibility in human pancreatic cancer cell lines to oncolytic virotherapy, when used under the same conditions. For this purpose, a distinct panel of purchasable human

pancreatic cancer cell lines was defined which resembles the spectrum of different subtypes of pancreatic adenocarcinoma.

Thus, this thesis was set out to contribute to the further development of the suicide gene “armed” virotherapy as a novel approach for the treatment of locally advanced or metastatic pancreatic cancer.

## 2. Material and Methods

### 2.1 Safety:

All experiments have been performed in a laboratory, that complies with biosafety level 2 (Directive 2000/54/EC – biological agents at work) from the European Parliament. All experiments with biological, potentially infectious or hazardous materials were performed under a hood, provided with laminar flow (HERAsafe®). No potentially infectious or hazardous biological material had left the laboratory. All biological material, that was no longer of use, was rendered harmless by sequential chemical disinfection, UV-light irradiation and additional autoclavation.

### 2.2 Material:

All mentioned materials have been used in the highest achievable purity. All products were stored according to manufacturer's recommendation at either room temperature, 4 °C or -20 °C. All used materials have been used in a sterile state, either by obtaining it directly from the stated companies or by former autoclavation at 2 bar with 121 °C for 20 minutes.

#### 2.2.1 Consumables:

| | |
|---|---|
| Cell scrapers | Corning Inc. |
| Cell strainer 40 µm | BD Falcon |
| Combitips 2.5 ml, 12.5 ml | Eppendorf |
| Conical-bottom tube 15 ml | Greiner Bio One |
| Conical-bottom tube 50 ml | BD Falcon |
| Cryotubes 1 ml | Corning Inc. |
| Latex gloves | Ansell |
| Pasteur pipettes, 230 mm long size | WU Mainz |
| Petri dish 10 cm | Greiner Bio One |
| Pipettes 1, 2, 5, 10, 25, 50 ml | Corning Inc. |
| Pipette tips 100 µl, 200 µl, 1000 µl, 1250 µl | Biozym / Peqlab |
| Nitrile gloves | Ansell |
| Reaction tubes 1.5 ml, 2.0 ml | Eppendorf |
| Reaction tubes 1.5 ml, 2.0 ml (amber) | Eppendorf |

| | |
|---|---|
| Syringes 1 ml, 10 ml | Braun |
| Tissue culture flask 75 cm², 150 cm² | Greiner Bio One |
| Tissue culture plate 12 / 24 / 96 well | Corning Inc. |

2.2.2 Laboratory equipment

| | |
|---|---|
| Autoclave 3850 EL | Systec |
| Digital camera, F-view | Soft Imaging Systems |
| Centrifuge | Eppendorf, Heraeus |
| FACSCalibur flow cytometer | Becton Dickinson |
| Haemocytometer | Hecht |
| HERASafe® workbench | Heraeus |
| Incubator | Heraeus / Integra / Memmert |
| IX50 inverted Fluorescence Microscope | Olympus |
| Multichannel pipette | Eppendorf |
| Pipette boy® | Integra |
| Phase contrast Microscope | Olympus |
| Refrigerator (-20 / -80 / -120°C) | Liebherr |
| Tecan GENios Microplate Elisa Reader | MTX lab Systems |
| Vacuum concentrator | Christ |
| Vortex mixer | Janke + Kunkel IKA Labortechnik |
| Water bath 3042 (37°C) | Köttermann |

2.2.3 Cell culture medium and buffer:

| | |
|---|---|
| Accutase | PAA Laboratories GmbH |
| Dulbecco's modified eagles Medium (DMEM) with stable L-glutamine with .5 g/l glucose | Biochrom AG |
| EDTA / Trypsin 0.05% | PAA Laboratories GmbH |
| Fetal bovine serum (FBS) | PAA Laboratories GmbH |
| PBS (cell culture use) | PAA Laboratories GmbH |
| RPMI 1640 | PAA Laboratories GmbH |
| ROTI®Block | Roth |

| | |
|---|---|
| Tween-20 | Roth |
| OPTI-MEM® | Gibco/ Invitrogen |

2.2.4 Chemicals

| | |
|---|---|
| 5-Fluorocytosine | Roche |
| 5-Fluorouracil | Roche |
| Acetic acid 1% (diluted from 100%) | Merck |
| Descosept AF | Dr. Schumacher GmbH |
| double distilled (dd)$H_2O$ | MilliQ Synthesis System |
| DMSO | AppliChem |
| Gamunex® 10% | Grifols Deutschland GmbH |
| Isopropranolol (70%) | SAV Liquid Production |
| Paraformaldehyde (PFA) 4% | Otto Fischar GmbH |
| NP40 lysis buffer | Invitrogen |
| Secusept | ECOLAB |
| Sulforhodamine B | Sigma |
| Trichloroacetic acid 10% | Roth |
| TRIS | Sigma |
| Trypan blue | Sigma |

2.2.5 Antibodies:

**Table 4a: Used primary antibodies for this dissertation.**

| Target | Dilution | Origin | Source |
|---|---|---|---|
| CD46 (human) | 1:20 in FACS buffer | mouse | eBioscience |
| IgG1 | 1:20 in FACS buffer | mouse | eBioscience |
| Vinculin (human) | 1:6.000 in Roti-Block | mouse | Sigma |
| SCD | 1:2.000 in Roti-Block | rat | Gifted from Transgene |
| MeV N-protein | 1:6.000 in Roti-Block | rabbit | Abcam |

**Table 4b: Used secondary antibodies for this dissertation.**

| Target | Description / name | Dilution | Origin | Source |
|---|---|---|---|---|
| Rat IgG | HRP conjugated | 1:30.000 Roti-Block | goat | Biorad |
| Mouse IgG | HRP conjugated | 1:30.000 | goat | Biorad |
| Rabbit IgG | HRP conjugated | 1:30.000 | goat | Invitrogen |

### 2.2.6 Used human pancreatic cancer cell lines

A pancreatic cancer cell line panel with 9 different, purchasable cell lines was defined (Table 5).

**Table 5: Cell lines used for this dissertation.** All cell lines were derived from patients, suffering from PDAC.

| Cell line name | Disease | Origin Host | Genetic alterations |
|---|---|---|---|
| AsPc-1 | Adenocarcinoma, metastasis: derived from ascites | female, 62 y.o. | CDKN2A, KRAS, MAP2K4, TP53 |
| BxPc-3 | Adenocarcinoma, primary site | female, 61 y.o. | BRAF, CDKN2A, SMAD4, TP53 |
| Capan-1 | Adenocarcinoma, metastasis: derived from liver metastasis | male, 40 y.o. | BRCA2, FZy/D10, GLT6D1, GRM1, KRAS, MAP2K4, SMAD4, SMAP2, TP53 |
| Capan-2 | Adenocarcinoma, primary site | male, 56 y.o. | CDKN2A, KRAS, TP53 |
| KP-3 | Adenosquamous carcinoma, primary site | male, 75 y.o. | KRAS, SMAD4, TP53 |
| KP-4 | Adenocarcinoma, metastasis: derived from ascites | male, 50 y.o. | KRAS |
| MIA-PaCa-2 | Adenocarcinoma, primary site | male, 65 y.o. | CDKN2A, KRAS, TP53 |

| | | | |
|---|---|---|---|
| Panc-1 | Adenocarcinoma, primary site | male, 56 y.o. | CDKN2A, KRAS, TP53 |
| T3M-4 (only used for GLV-1h94) | Adenocarcinoma, metastasis: derived from lymph node | male, 64 y.o. | KRAS, TP53 |

The cells are of different origin (primary site vs. metastasis) and with KP-3 feature also of different morphological characteristics. The panel was sought out to resemble the tumor-heterogeneity of pancreatic cancer. Most cell lines feature the typical KRAS- and TP53-mutation, whereas some didn't.

The KP-3 and KP-4 cell lines were gifts from *Prof. Ruben Plentz* and his group in Tübingen. The T3M-4 cells was a gift from *Prof. Guy Ungerechts* and his group in the NCT, Heidelberg. As the T3M-4 cells were received when all experiments with MeV-SCD already had been accomplished, T3M-4 cells solely were used in the context of measurement of GLVh194 oncolysis.

Cell lines were cultivated in either DMEM or RPMI medium, supplemented with 5 % or 10 % fetal bovine serum (FBS) and kept in 75 cm 2 tissue culture flasks with vented caps. Flasks were stored in incubators at 37 °C in a humid atmosphere, containing 5 % $CO_2$. Treatment was done under sterile conditions in a HERAsafe® workbench.

### 2.2.7 Oncolytic measles vaccine viruses MeV-SCD and MeV-GFP

MeV-SCD was generated and provided by Wolfgang Neubert. It has already successfully been used for *in vitro* treatment of cholangiocarcinoma (Lange et al., 2013), ovarian cancer (Hartkopf et al., 2013) or acute myeloid leukemia (Maurer et al., 2019). MeV-SCD and MeV-GFP were genetically modified either by insertion of the SCD "suicide-gene" *or* green fluorescent protein (GFP) at the 3'-lead position (*Fig. 9*).

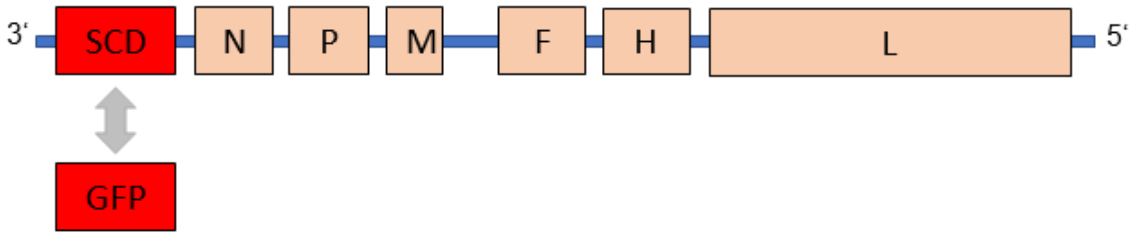


**Fig. 9: Schematic representation of linear MeV-SCD / -GFP negative strand RNA-genome.** SCD/GFP transgene colored in red have been inserted in the leading position, hence using the transcription gradient for maximal transcription.

MeV-GFP was used only for evaluation of MeV primary infection rate. All further experiments were done using MeV-SCD.

2.2.8 Oncolytic vaccinia virus GLV-1h94

GLV-1h94 was kindly provided by Genelux Corporation, San Diego, California, USA. It was originated from the *Lister* strain of vaccinia virus and genetically modified by inserting three different transgenes into the viral genome (*Fig. 10*):

1. By inactivation of the gene locus F14.5L, a gene encoding for a fusion protein, consisting of *Renilla* luciferase and *Aequorea*-Green fluorescent protein was inserted. Transcription is initiated by the promoter of the early- and late-gene group ($P_{SEL}$). The inserted gene function as a marker gene, as it allows visualization of viral replication on a cellular level.
2. The J2R (thymidine kinase gene) was inactivated by the insertion of lacZ (encoding beta-galactosidase, under the control of vaccinia virus Western Reserve early/late p7.5 promoter) and hTFR (human transferrin receptor cDNA, inserted in the reverse orientation to pSEL, therefore hTFR is not expressed). The inserted genes allow quantifiable measurement of transgene-expression as surrogate parameter for viral infection.
3. The A56R (hemagglutinin gene) was inactivated by the insertion of fcu1, encoding for the super cytosine deaminase (SCD), a fusion protein consisting of yeast cytosine deaminase and uracil phosphoribosyl transferase, the same prodrug-convertase system as in MeV-SCD. Transcription is again initiated by $P_{SEL}$.

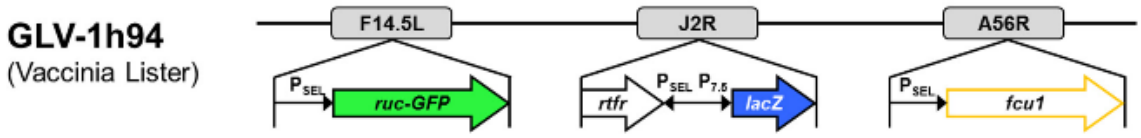


**Fig. 10: Schematic representation of a selected region of interest of the linear GLV-1h94 DNA-genome.** Modified gene-loci highlighted in grey; inserted transgenes depicted underneath (Berchtold et al., 2020).

## 2.3 Methods

### 2.3.1. General cell culture:

Cells were cultivated in either DMEM or RPMI medium. Fetal bovine serum (FBS) in either 5 or 10 % was added to culture medium for supplementation. Cell cultures were kept in 75 $cm^2$ tissue culture flasks with vented caps. Flasks were stored in incubators at 37 °C in a humid atmosphere, containing 5 % $CO_2$ and at least 95 % humidity. The cell culture was kept under sterile conditions in a HERAsafe® workbench, provided with laminar flow.

To prevent overgrowth, the confluence of the cell layer in the cell culture flasks was controlled once daily through phase contrast microscopy at 4x magnification. Cells were approximately passaged 2-3 times a week, depending on used cell line, when cell layer was almost confluent.

Cell debris was removed before each passage by rinsing with 10 ml PBS at 37 °C. After removal of buffer/cell debris overlay, the cells were detached from flask bottoms by application of 2 ml Trypsin. Trypsin was inactivated by application of fresh FBS-supplemented medium. Cell suspension was filtered through a 40 µm cell strainer, if needed. Depending on growth rate of used cell line, $^1/_{10}$ to ¼ of original cell mass, was kept for further cultivation.

### 2.3.2. Cryoconservation and thawing of cells:

Cells were rinsed, trypsinized and suspended in cell culture medium as described under 2.3.1. Suspension was centrifuged at 210x g and supernatant consecutively removed. The so generated cell pellet was resuspended in freezing medium with DMEM supplemented with 20 % FBS and 10 % DMSO and applied to cryotubes with quantity of approximately $10^6$ cells / ml / aliquot. Cryotubes were

frozen slowly down to -80 °C, protected by a styrofoam box. After 24 hours, the cryotubes were transferred and stored finally in a -140°C freezer.
For thawing, the cryotubes were transferred from the freezer to a water bath and cautiously heated. The 1 ml aliquots were suspended in 9 ml of preheated DMEM and centrifuged at 1200 rpm for the duration of 2 minutes. Supernatant was discarded in order to remove cytotoxic DMSO from the new cell culture and cell pellet was resuspended in preheated DMEM and transferred to a new culture flask.

2.3.3. Determination of the cell count:

Counting of suspended cells was done by using an improved Neubauer haemocytometer (*Fig. 11*). Each large quadrant in every corner of the Neubauer haemocytometer is 1 mm². Each quadrant is divided into 16 smaller squares.

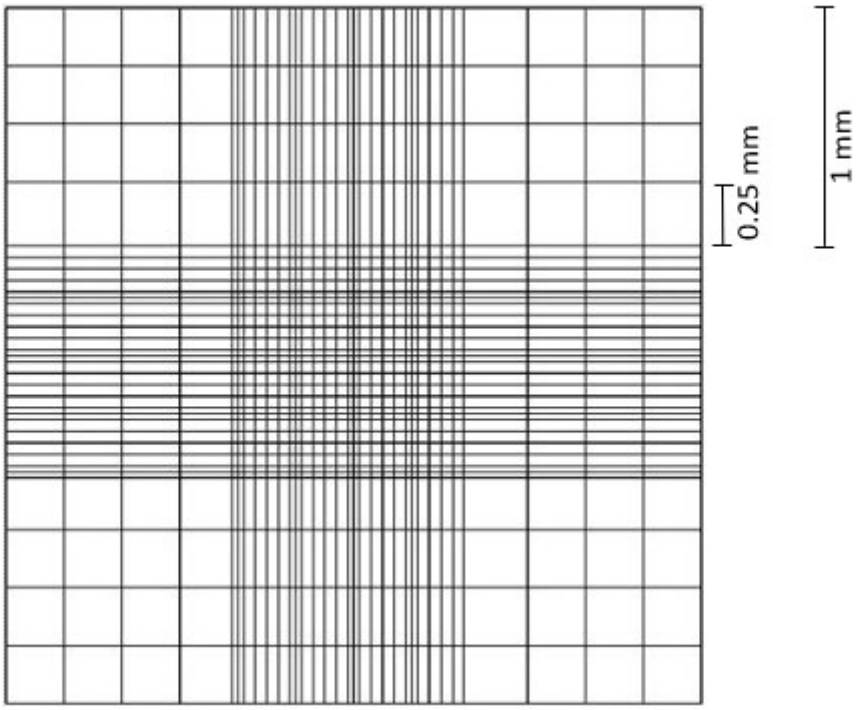


Fig. 11: Schematic representation of Neubauer counting chamber. Each larger quadrant in every corner of the counting chamber is 1 mm².

For cell counting, 10 µl of cell culture flask solution was suspended with 90 µl trypan blue (1:10), then applied to each larger quadrant. Trypan blue is used to rule out dead cells, as only dead cells would be susceptible to trypan-blue

staining. An intact cell membrane would prohibit trypan-blue uptake into the vital cell.

To determine the number for cells per ml in the cell suspension, the number of vital cells was counted for each larger quadrant. This was done by phase contrast microscopy with 10x magnification. The arithmetic mean of all 4 quadrants was calculated and multiplied by 10.000. This equals the number of cells per ml. Trypan-blue stained dead cells were excluded.

$$\frac{cells}{ml} = \frac{all\ counted\ cells}{quadrants}\ \mathrm{x}\ 10^5$$

2.3.4 Cell exposure to 5-fluorouracil:

As the used viruses encode for a cytosine-deaminase protein, being able to convert 5-fluorocytosine (5-FC) into 5-fluorouracil (5-FU) to enhance the oncolytic activity, it was needed to examine whether the used cell lines were susceptible to 5-FU treatment in the first place. For this purpose, all cell lines were exposed to different 5-FU concentrations. Susceptibility to 5-FU was defined as reduction of cell mass by 50 %, compared to untreated control.

Cells were detached from culture flasks as described in 2.3.1 and counted as described in 2.3.3. 3 x $10^4$ cells were seeded in each well of a 24-well plate and incubated for safe adherence overnight. The following day, the culture medium of quadruplicates was replaced by medium containing 5-FU with concentrations ranging from 1 nmol/l to 1 mmol/l. The cells were incubated with the 5-FU containing medium for 72 hours. Remaining cell viability was measured using Sulforhodamine B viability assay (see chapter 2.3.9).

2.3.5. Multiplicity of infection (MOI):

Multiplicity of infection (MOI) is a standardized virological term to define a number of infectious viral particles in relation to a defined number of recipient cells in a culture.

$$MOI = \frac{volume\ (virus) x\ concentration\ (virus)}{volume\ (cell\ culture) x\ concentration\ (cell\ culture)}$$

A MOI of 1 resembles one viral particle for every cell, that could possibly get infected. A MOI of 0.1 would resemble one viral particle for every 10 cells.

2.3.6. Controlled viral infection:

Cells were detached from culture flasks as described in 2.3.1 and counted as described in 2.3.3. 3 x $10^4$ cells were seeded in each well of a 24-well plate and incubated for safe adherence overnight. The following day, the needed virus stock (either MeV-SCD, MeV-GFP or GLV-1h94) was carefully thawed and vortexed, as it was stored in a frozen condition. Thawed virus was diluted in preheated OPTI-MEM to the necessary titer, depending on the required MOI and added to the well plate in the same concentration for each column (*Fig. 12*).

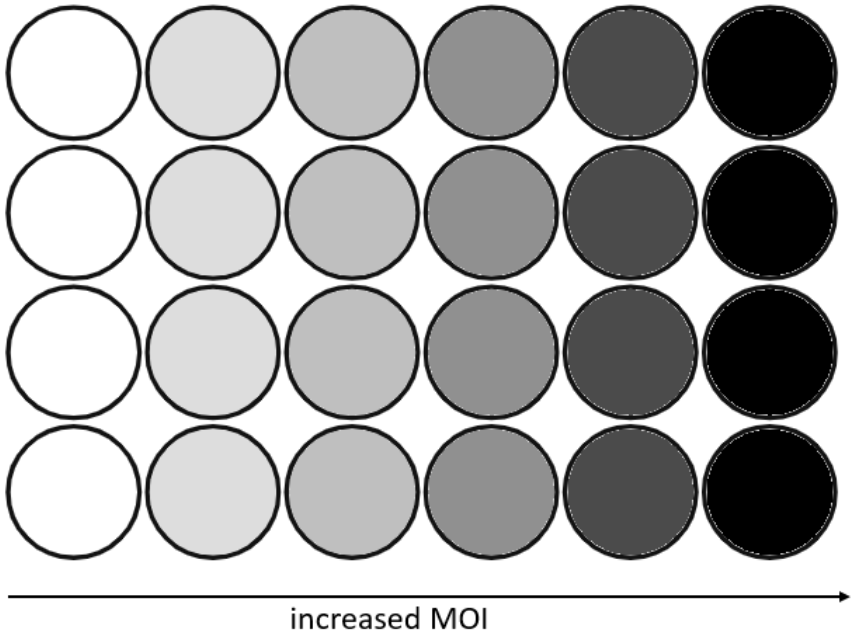


**Fig. 12: Schematic representation of a 24-well plate, used for viral infection.** Shades of grey resemble increasing viral concentration, measured in MOI. White wells serve as negative control. Each column, shaded in the same color, share the same MOI. Only arithmetic mean of quadruplicates, infected with the same MOI were accounted for results.

The used virus was incubated at 37 °C with the cells and gently moved every 20 minutes to provide equal viral spread as possible. Depending on the used virus,

at 3 hours post infection (hpi) (MeV) or 1 hpi (VACV), the virus-containing overlay was removed and cells were again incubated at 37 °C with preheated DMEM. The negative control was mock treated with PBS. The incubation time of the virus-infected cells ranged from 24 to 96 hpi, depending on the assay. Quantification of cell viability was done by SRB assay (see chapter 2.3.9); quantification of MeV-GFP primary infection rate was done by flow cytometry (see chapter 2.3.10).

### 2.3.7. Application of prodrug 5-fluorocytosine to infected cells

In order to evaluate the enhancement of the oncolytic effect of the usage of the prodrug-convertase system in MeV-SCD and GLV-1h94, the infected cells were incubated with 5-FC containing medium.

For this assay, cells were distributed and infected with the virus, as described in 2.3.6. After removal of the virus-containing overlay, the cells were further incubated at 37 °C with medium containing 1 mM of 5-FC for another 96 hpi. Remaining cell viability was measured using SRB-viability assay (see chapter 2.3.9).

### 2.3.8. Fluorescence microscopy

To document and visualize the viral infection throughout the different cell lines, fluorescence enhanced microscopy was performed at 24 and 48 hpi with different MOIs. This experiment was done using MeV-GFP.

Cells were detached from culture flasks as described in 2.3.1 and counted as described in 2.3.3 and seeded in each well of a 24-well plate. The cells were infected with MeV-GFP as described in chapter 2.3.6. MOIs ranged from 0.01 to 10. PBS-treated cell lines served as control (mock). At 24 and 48 hpi, regular phase contrast microscopy was performed and several pictures were taken (location randomly assigned within the well) of the cell layer with an inverted microscope (Olympus IX 50), equipped with a digital camera (F-view, Soft Imaging System GmbH). With a 100 W light source (Olympus U-RFL-T), the exact same loci were exposed to filtered light with a wavelength of 489 nm. GFP fluorescence was measured at its peak with 508 nm (Tsien RY, 1998). Pictures of the corresponding sites were taken with the same equipment.

### 2.3.9. Sulforhodamine B (SRB) cell viability assay

The SRB assay is a standardized cell viability assay, which can quantify viable, adherent cell mass at a certain time point and therefore conversely can measure the cytotoxic effect of a substance (Skehan et al., 1990). This assay was used to determine cell viability after viral infection, viral infection with added prodrug 5-FC and after exposure to 5-FU. SRB-based dye is an anionic protein dye, which binds to basic amino acids, e.g. of cellular proteins under acidic conditions, induced by trichloroacetic acid (TCA). The amount of SRB-colored cellular protein serves as a surrogate parameter for remaining, viable cell mass. The quantity of dyed protein correlates linear with the colorimetric extinction measured by a photometer.

For SRB assay, the cells in the 24-well plates were initially pretreated by removal of medium / overlay and then rinsed with 4 °C PBS. This was done to remove debris and dead cells from the wells. After rinsing, the plates were incubated with TCA for 30 minutes at 4 °C, resulting in a strong adherence of the (former) viable and now fixed cells to the well plate. The well plates were now washed with regular tap water, at least 4 times to remove remaining TCA and remaining debris from the plate. Plates were consecutively dried at 40 °C overnight and the now fixated cells / well plates could theoretically be stored limitless for further analysis. Usually, the following day, the cells were stained by application of 250 µl of SRB-staining solution to each well for 10 minutes. In order to remove abundant SRB-staining solution, the well plates were washed with 1 % acetic acid until the washout became visibly clear. Afterwards, the plates were dried and the now SRB-stained, fixated cell layer in each well was dissolved in 1 ml of 10 mM TRIS base solution. 80 µl of each well was now transferred to a 96-well plate in duplicates. The ELISA reader (Tecan Genios Plus) could now measure photometrical extinction at 564 nm wavelength, which correlates with remaining cell mass in the examined well.

Results were depicted in percentage by comparison to mock-treated wells, as absolute cell mass differed substantially in used cell lines.

### 2.3.10. Flow cytometry

For determination and quantification of CD46 surface expression, flow cytometry was used for each used pancreatic cancer cell line.

Cells were incubated at 37 °C with preheated PBS (cell culture use), 12 h before experiment. In contrast to cell culture, 1 ml Accutase® was used, instead of trypsin for detachment. Detached cells (1 ml) were suspended with 3 ml FACS-buffer (PBS, added with 10 % FBS) and centrifuged at 210 x g for 4 minutes. Supernatant was discarded, and cell pellet again suspended in FACS-buffer. Cells were counted as described in 2.3.3 and 5 x $10^5$ cells were diluted in 3 ml PBS and again centrifuged at 4 °C at 472 x g for 5 minutes. Supernatant was again discarded and cell pellet was added with 10 µl Gamunex® 10%, to block Fc-terminals for unspecific binding and resuspended in 50 µl FACS buffer. New suspension was incubated for 5 minutes on ice. Then, 2.5 µl of either a PE-conjugated human CD46 antibody or 2.5 µl of a PE-conjugated mouse IgG1-isotype control was added and incubated for further 30 minutes on ice.

Finally, the now stained cells were again diluted in 4 ml PBS and once more centrifugated at 4 °C at 472 x g for 5 minutes. Cell pellets with stained cells were resuspended in 500 µl FACS-buffer and measured by the flow cytometer FACSCalibur (Becton Dickinson). Results were calculated and graphically depicted with WinMDI software.

Flow cytometry was also used for quantification of MeV-GFP primary infection rates. MeV-GFP infected cells were conditioned as described above. As MeV-GFP infected cells emit fluorescence by GFP expression, cells didn't have to be stained by antibodies and could therefore directly be measured in the flow cytometer. Again, results were calculated and graphically depicted with WinMDI software.

### 2.3.11. Western blot analysis

To determine and quantify protein expression over time of wild type viral genes and inserted transgene, western blot analysis was performed.

*Preparation of cell lysates*

Cells were detached from culture flasks as described in chapter 2.3.1 and counted as described in chapter 2.3.3. 2 x $10^6$ cells were suspended in 8 ml DMEM and transferred to a 10 cm petri dish. After established cell adherence the next day, the cell layer was rinsed with 8 ml of preheated PBS (cell culture use) and then infected with MeV-SCD at MOI 1, as described in chapter 2.3.6. Cells were lysed at 24, 48, 72 and 96 hpi in 500 µl NP40 lysis buffer, scraped off the petri dish and transferred into a 1.5 ml reaction tube. Cell-suspension was now subsequently frozen and thawed three times in a row, by shock-frosting in liquid nitrogen, followed by thawing in a heating block at 37 °C. The cell suspension was ultimately centrifuged at 16.000 x g at 4 °C for 10 minutes, allowing the protein-containing supernatant to be separated, collected and transferred to a new reaction tube.

*Measurement of protein content by Bradford dye assay*

To determine protein content of supernatants, proposed for western blot analysis, the Bradford dye assay was performed with Bio-Rad protein assay kit (Bio-Rad Laboratories GmbH).

A standard curve was established by diluting a bovine serum albumin (BSA, 10 mg/ml) stock solution, serving as control, into following concentrations: 0.05, 0.1, 0.25 and 0.5 mg/ml in dd$H_2O$. Bradford dye reagent was diluted 1:5 in dd$H_2O$; protein-containing supernatants were diluted 1:50 and 1:00 in dd$H_2O$. 10 µl dd$H_2O$ and 10 µl of each dilution, were transferred to a 96-well plate in duplicates. In each well 200 µl of Bradford dye was added. The ELISA reader (Tecan Genios Plus) could now measure photometrical extinction at 595 nm wavelength. The optical density of the different, defined BSA concentrations served to generate a standard curve, from which protein content of the supernatants could be calculated.

*Sodium dodecyl sulfate-polyacrylamide gel electrophoresis (SDS-PAGE)*

SDS-Page is a well-known, standardized technique to separate different proteins, based on their molecular weight, using electrophoresis in a polyacrylamide-based matrix (Laemmli UK, 1970).

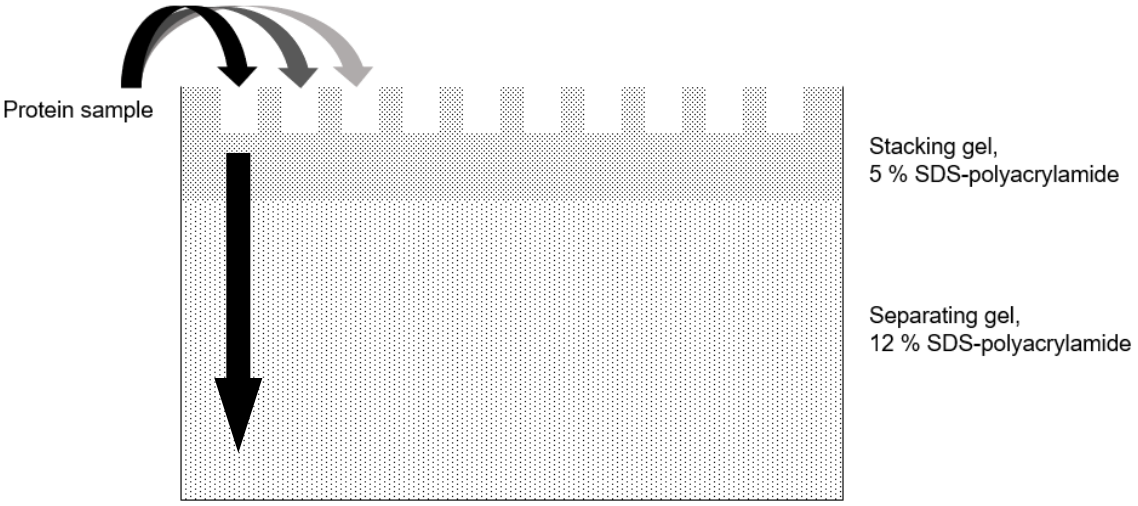


**Fig. 13: Schematic representation of an electrophoreses gel cassette, filled with separating- and stacking SDS-polyacrylamide gel.** Protein samples are placed in slots, as depicted and by application of voltage, migrate into the separating gel (velocity determined by molecular weight).

For this dissertation, a 12 % polyacrylamide gel as separating and a 5 % polyacrylamide gel as stacking gel were used for the experiments (*Fig. 13*). The following table shows the composition of the used gels:

| Substance | Stacking gel (12 %) | Separating gel (5 %) |
|---|---|---|
| Acrylamide 30 % | 0.33 ml | 4.0 ml |
| APS 10 % | 0.02 ml | 0.1 ml |
| $ddH_2O$ | 1.4 ml | 3.3 ml |
| SDS 10 % | 0.02 ml | 0.1 ml |
| TEMED | 0.002 ml | 0.004 ml |
| Tris (pH 6.8) 1 M | 0.25 ml | - |
| Tris (pH 8.8) 1.5 M | - | 2.5 ml |

The 12 % separating gel was produced according formula depicted in the table above. The separating gel was filled into the gel cassette of the electrophoresis device and covered immediately with isopropanol 70 % to level gel surface. After 30 minutes, the polymerization of the gel matrix was finished and the isopropranol could be removed. The surface was now washed with $ddH_2O$. The stacking gel 5 % was produced according to formula depicted in the table above and cast into the gel cassette on top of the separating gel. By using a comb, 10 slots were formed during 20 minutes polymerization of the stacking gel. The now prepared gel cassette was placed inside the buffer tank, filled up and covered with buffer solution (Tris 125 mM + Glycine 950 mM + SDS 0.5 %).
Protein-containing supernatant, measured and calculated as described in chapter 2.3.12, was heated to 95 °C for 5 minutes in order to disrupt secondary or tertiary protein structures, which would hamper the analysis. After removal of the comb, 75 µg of each sample was placed in one of the preformed slots inside the stacking gel. With application of 100 V voltage to the electrophoresis device, the proteins migrate through the separation gel with different velocity, based on molecular weight. Small proteins move faster than large proteins. The proteins therefore get separated, based on their molecular weight.

*Western blotting*

After separation of the proteins in the SDS-polyacrylamide gel matrix, the proteins are transferred from the separation gel to a polyvinylidene difluoride- (PVDF) membrane. This was done by electroblotting. The PVDF-membrane was placed on the separating gel layer, embedded between two Whatman (filter) papers on each side, covered with a sponge on each side. The whole sandwich-like composition is held together tightly by a pressure-applying device and soaked in transfer-buffer (Tris 48 mM + Glycine 39 mM + Methanol 20 %). By application of voltage, the proteins are perpendicularly blotted onto the PVDF-membrane. To control successful blotting, the PVDF-membrane was stained with Ponceau-S solution (Ponceau-S 0.1 % + acetic acid 5 %), which reversibly binds to positively charged amino-groups of proteins. Ponceau-S solution is highly water-soluble and staining was reversed by washing the PVDF-membrane with $ddH_2O$.

To visualize and identify the now separated and blotted proteins, immune-staining was performed. The protein-sample containing PVDF-membrane was covered in a milk solution (milk powder 5 % + TBS-Tween) in order to prevent unspecific antibody-binding. Afterwards, the membrane was washed twice in a TBST solution (TBS pH 7.4 + Tween, 0.02 %) and cut into sections, containing only one protein band. The primary antibodies (anti-SCD, anti-Vinculin, anti-N-Protein) were diluted in Roti-Block and separately applied to the different membrane sections. After overnight incubation at 4 °C on a shaker, the antibody solutions were removed and washed three times with TBST for five minutes. The secondary antibodies (horseradish peroxidase (HRP) labeled) were also diluted in Roti-Block. Each secondary antibody-solution was incubated with its membrane section for one hour at room temperature on a shaker. The membrane sections were once more washed with TBST for 10 minutes. The protein bands were visualized via enhanced chemiluminescence (ECL). The membrane sections were incubated with 1 ml ECL solution for three minutes and afterwards fixed in a photo cassette (Dr. GOOS Suprema Universal 100).

Finally, the cassettes / membrane sections were exposed to the high performance chemiluminescence film (Amersham Hyperfilm ECL, GE Healthcare ltd.).

## 3. Results

### 3.1 Oncolytic measles vaccine virus (MeV-SCD)

#### 3.1.1. CD46 expression of pancreatic cancer cell lines

CD46 constitutes the viral entry receptor for measles vaccine virus. *Fig. 14a* shows the expression rate of CD46 on the surface of all eight tested human pancreatic cancer cell lines originating from different types of pancreatic cancers (see *table 1*). Via flow cytometry it could be demonstrated that all of the analyzed pancreatic cancer cell types do express CD46. This also revealed that there are gross differences in levels of CD46 expression between the used different cell lines indicated by differences in index-numbers (arithmetic mean of anti CD46 / isotype control) ranging from 20.9 for Capan-1 cells (derived from liver metastasis) up to 55.7 for Panc-1 (derived from epitheloid pancreatic carcinoma).

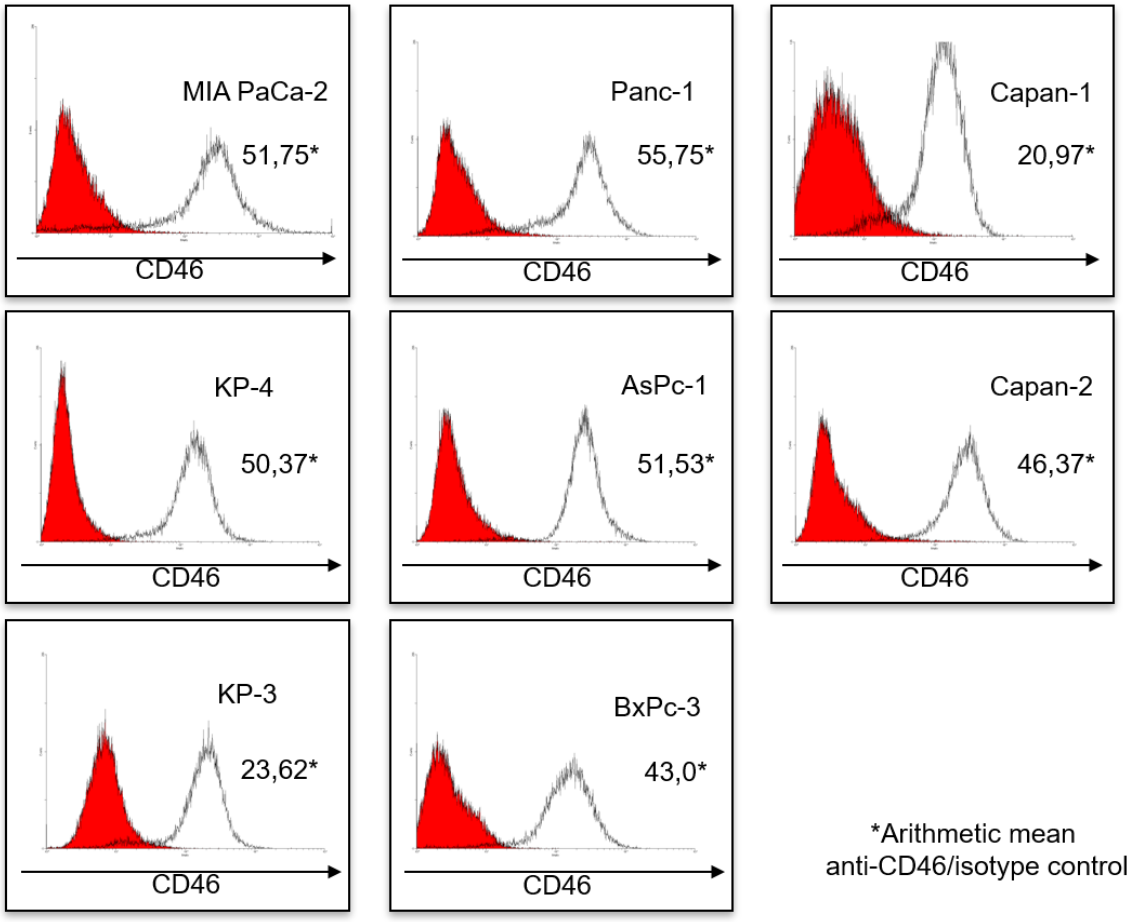


**Fig. 14a: Human pancreatic cancer cell lines express high levels of CD46 receptors on their surfaces.** Cells were stained with anti-CD46 antibody (white histogram) or an isotype control (red histogram) and analyzed by flow cytometry. The

depicted number shows the ratio of the mean fluorescence index of the ratio white histogram/red histogram. An arithmetic mean under 20 is considered as marginal CD46 expression on the cell surface.

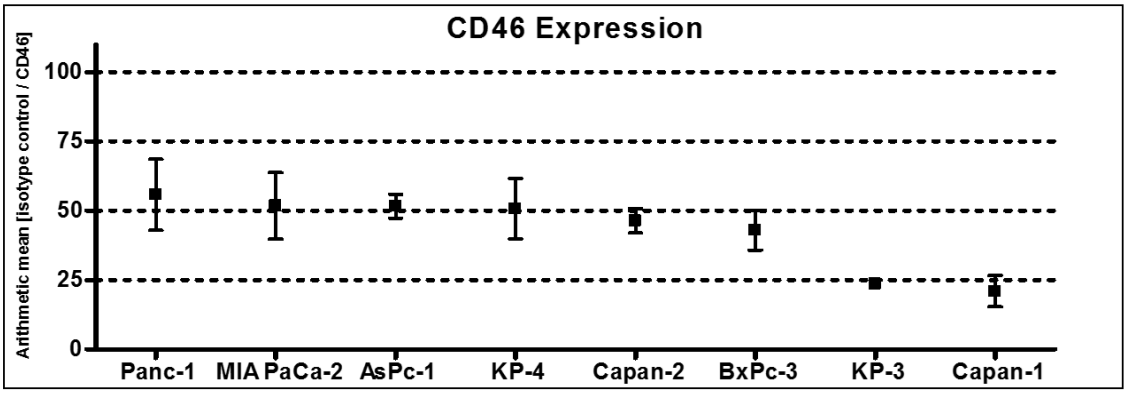


**Fig. 14b: CD46 expression rates of all tested human pancreatic cancer cell lines** (aligned from highest to lowest expression levels).

These results, summarized in *Fig. 14b*, indicate that human pancreatic cancer cell lines express high amounts of the measles vaccine virus entry receptor and therefore are expected to be susceptible without exception to oncolytic measles vaccine virus infection. In addition, it can be assumed that viral spreading from infected to hitherto uninfected tumor cells might be differentially effective depending on the CD46 expression rate of the respective human pancreatic cancer cell line under investigation.

### 3.1.2. Primary infection rate of MeV-GFP

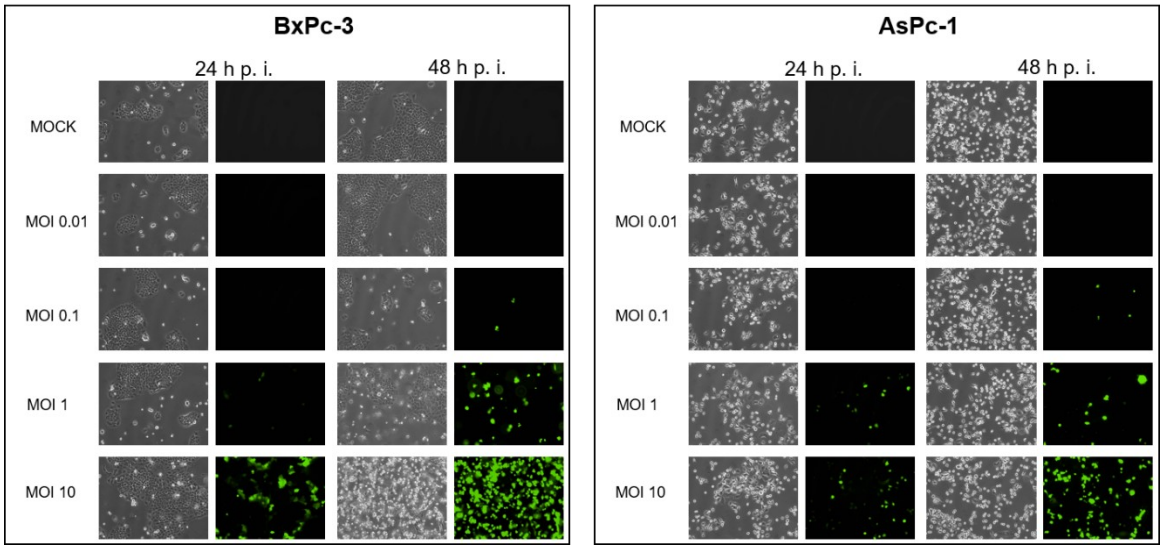

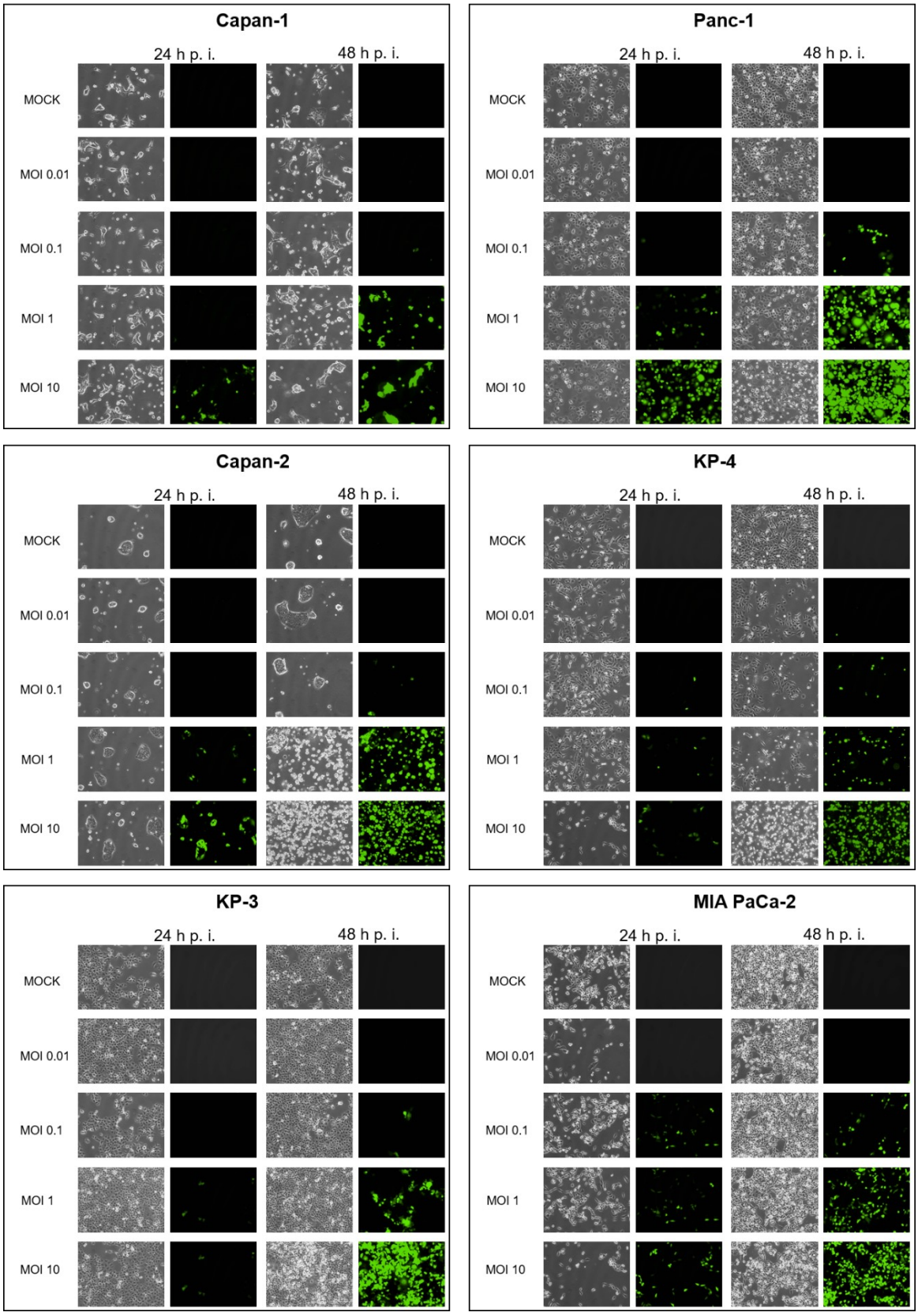


**Fig. 15a: Primary infection rates of MeV-GFP in PDAC cell lines.** All eight tested human pancreatic cancer cells were incubated with a measles vaccine virus encoding the GFP marker gene, MeV-GFP, at different viral concentrations (MOI - multiplicities of

infection) and compared with untreated controls (MOCK). Pictures were taken via fluorescence microscopy at 24 and 48 hours post infection (hpi).

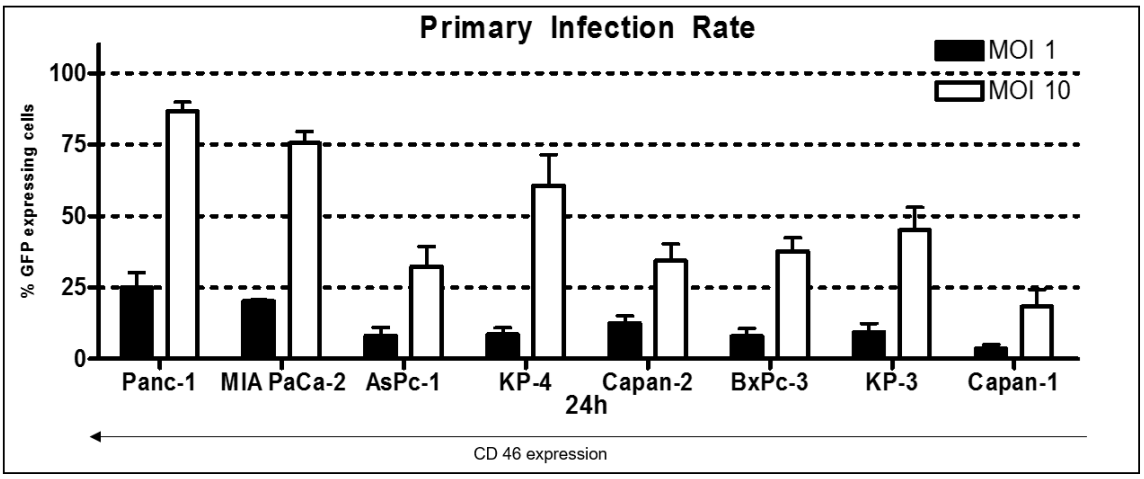


**Fig. 15b: Primary infection rates of all eight tested human pancreatic cancer cell lines at 24 hours post infection (hpi) with MeV-GFP, analyzed via flow cytometry.** At 24 hpi, not much replication of MeV-GFP has taken place, but expression of MeV-GFP marker gene GFP already has been functional; therefore, levels of GFP expression obtained at 24 hpi reflect the amount of infectious viral particles being taken up by the target cells. Black bars depict results obtained at multiplicities of infection of 1 (MOI of 1; meaning employment of 1 infectious viral particle per targeted cancer cell), whereas white bars show results obtained at MOI of 10. Pancreatic cancer cell lines are aligned from left to right displaying highest to lowest expression levels of CD46 at MOI 1 and 10.

All tested human pancreatic cancer cell lines were susceptible to measles vaccine virus infection. The primary infection rate was dependent on time **(**extension of time period to 48h**)** and quantity of viral particles used for infection (compare results obtained with MOI 1 versus MOI 10). For measurement of the infection rate, MeV-GFP was used. In *Fig. 15a,* viral spreading is depicted via fluorescence microscopy using Panc-1 tumor cells, exhibiting a much higher level of CD46 expression in comparison to cell line Capan-1. Results being obtained primarily optically by fluorescence microscopy were further quantified via flow cytometry (see *Fig. 15b*). 24 hpi, using a MOI of 1, primary infection rates were found to range from 24.9 % for Panc-1 to 3.6 % for Capan-1. As expected, infection rates were found to be increased using a higher MOI of 10.

### 3.1.3 Cytotoxic effect of 5-FU on pancreatic cancer cell lines

The used oncolytic virus MeV-SCD encodes the highly active suicide gene SCD (comprising a fusion of a yeast cytosine deaminase and a yeast uracil phospho-

ribosyltransferase) which enables infected tumor cells to convert the non-toxic prodrug 5-FC into 5-FU intracellularly. Sulforhodamine-B (SRB) viability assays were performed to analyze the cytotoxic effect of different concentrations of 5-FU on the defined panel of eight human (uninfected) pancreatic cancer cell lines (see *Fig. 16*).

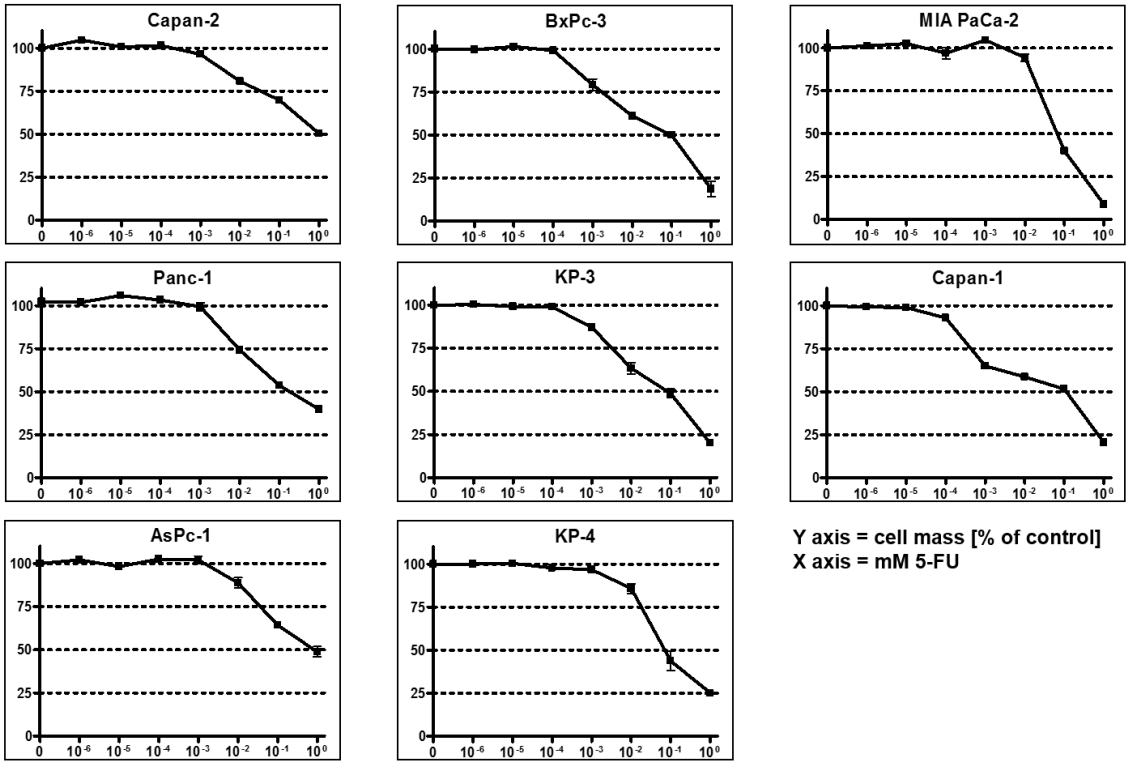


**Fig. 16: SRB tumor cell viability assay with all eight tested human pancreatic cancer cell lines being performed at 72 hours of exposure to 5-FU (at concentrations ranging from 1 nmol/l to 1 mmol/l).**

These experiments showed that 5-FU is able to kill human pancreatic cancer cells in a dose-dependent manner. In all tested cell lines, 5-FU concentrations greater than 0.1 mmol/l were needed to decrease tumor cell viabilities to less than 50 % in comparison to the controls (*Fig. 16*). Interestingly, the susceptibilities of the pancreatic cancer cell lines to 5-FU treatment were not found to correlate with CD46 expression nor with MeV-SCD infection rates.

### 3.1.4. Oncolytic effect of MeV-SCD on pancreatic cancer cell lines

In order to determine the oncolytic potential of MeV-SCD, the used cell lines were infected with MeV-SCD for 96 hpi and additional treated with or without the prodrug 5-FC (*Fig. 17a*).

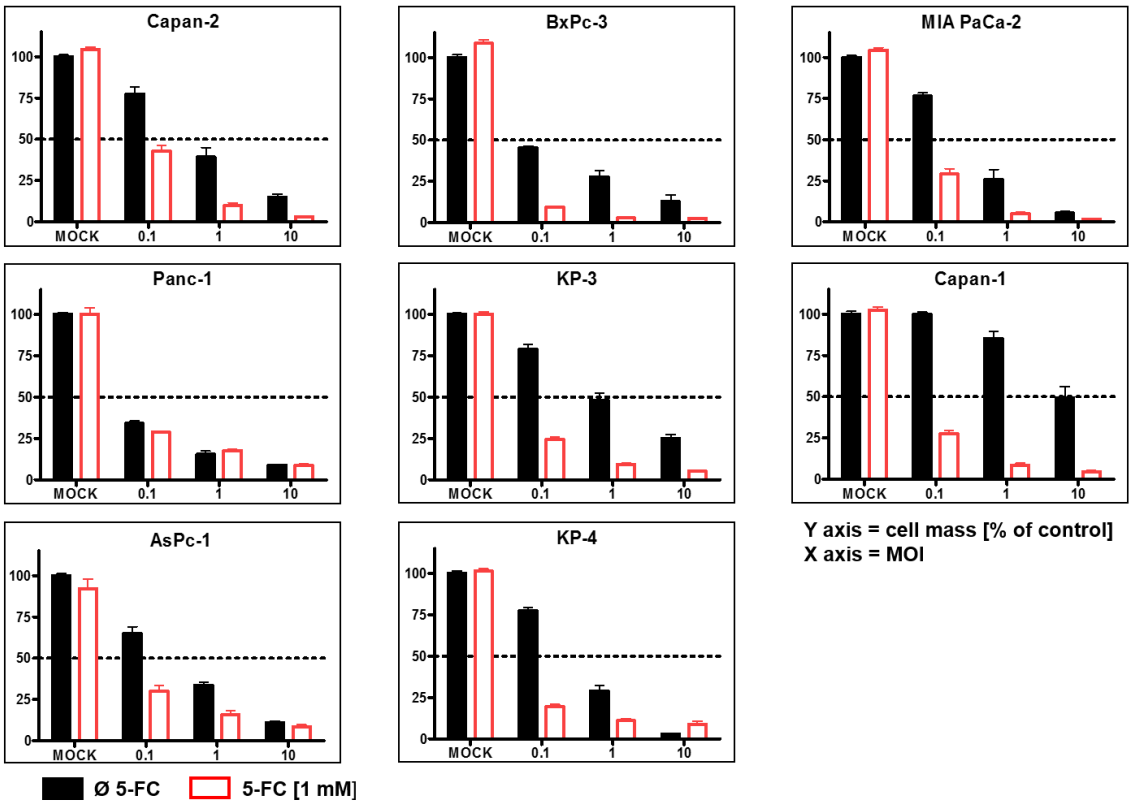


**Fig. 17a: SRB-viability assays at 96hpi with MeV-SCD with and without addition of the prodrug 5-FC.** Viral concentration ranges from MOI 0 (MOCK control), 1 to 10. Primary resistance to the oncolytic effect (horizontal dotted line) is defined by a remaining cell mass > 50 % of control at MOI 1, 96 hpi.

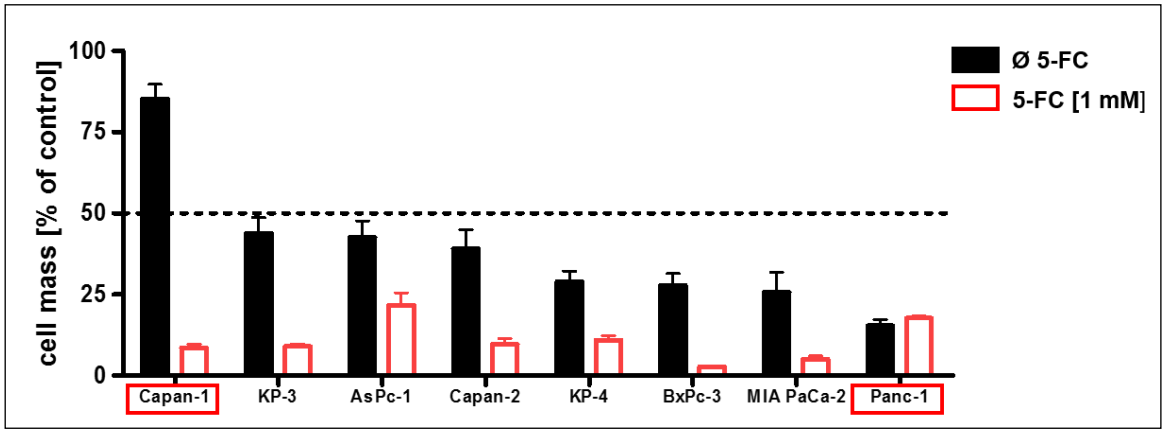


**Fig. 17b: Response to MeV-SCD-mediated oncolysis.** All eight cell lines of the used panel of human pancreatic cancer cell lines were infected with MeV-SCD (MOI 1) and

incubated at 3 hpi with or without the prodrug 5-FC (1 mM). At 96 hpi, tumor cell viabilities were quantified using the SRB viability assay. Alignment of the eight human pancreatic cancer cell lines from weakest (to the left) to strongest (to the right) oncolytic effect. The dotted horizontal line marks the cutoff being used for definition of primary resistance to MeV-SCD oncolysis, i.e. more than 50 % viable tumor cells at 96 hpi in comparison to uninfected control tumor cells (MOCK).

All eight tested human pancreatic cancer cell lines were responsive to MeV-SCD mediated oncolysis, albeit in a dose dependent manner (see *Fig. 17a*). Interestingly, seven out of eight tumor cell lines showed less than 50 % viability at 96 hpi without additional application of the prodrug 5-FC. Only one tumor cell line, Capan-1, displayed a high primary resistance to oncolysis by MeV-SCD with a viability rate > 75 % at 96 hpi. With addition of the prodrug 5-FC, the oncolytic effect was significantly enhanced in seven out of eight tumor cell lines. Only in Panc-1 tumor cells, addition of 5-FC had no additional beneficial effect; however, Panc-1 tumor cells had been found to be already very susceptible to MeV-SCD displaying the largest reduction in tumor cell mass at 96 hpi in absence of 5-FC; therefore, it was not expected that addition of 5-FC could enhance the extent of tumor cell destruction any further.

### 3.1.5. Kinetics of MeV-NP and SCD expression in the course of infection with MeV-SCD

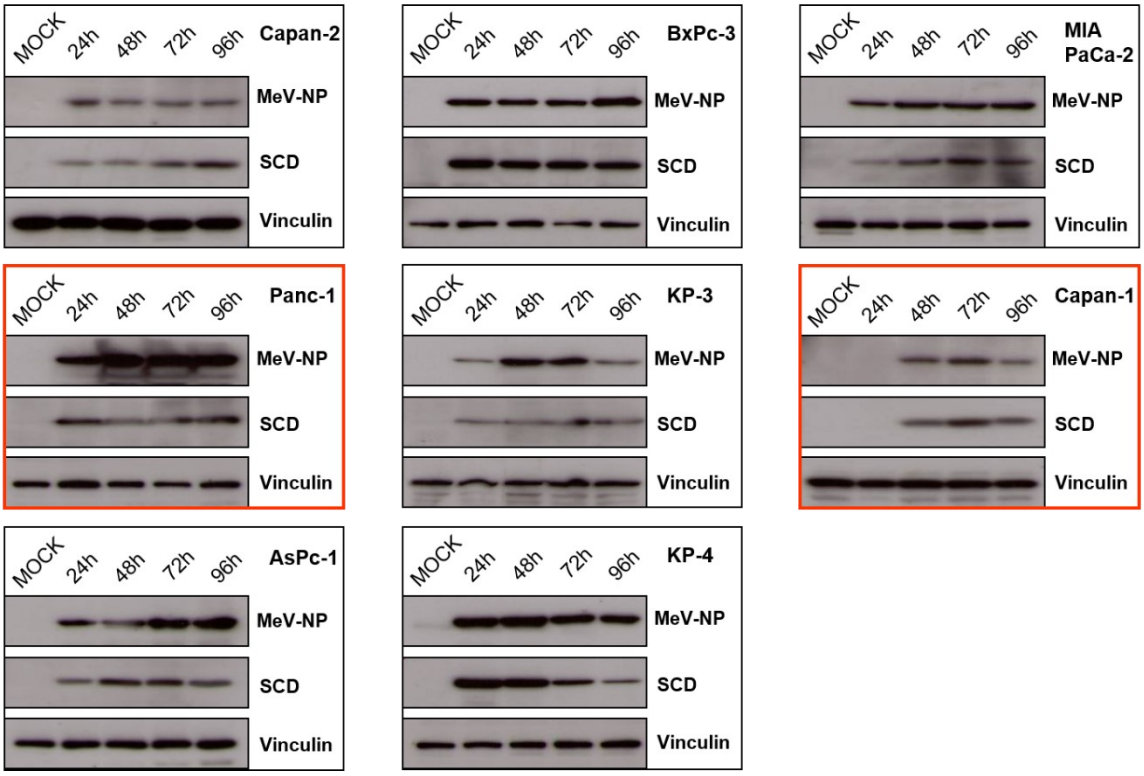


**Fig. 18: Western blot analysis showing expression of MeV-NP (60 kDa) and SCD (35 kDa) at 24, 48, 72 and 96 hpi with MeV-SCD.** In contrast to mock treated cells, all infected (MOI 1) cell lines did express wild-type viral (MeV-NP) and inserted transgene encoded (SCD) proteins. Viral protein expression differed from high expression already at 24 hpi (e.g. Panc-1) to low / moderate expression beginning at 48 hpi (Capan-1); both cell lines highlighted in red. Vinculin (115 kDa) served as control.

In order to confirm the principle of enhanced MeV-SCD-mediated oncolysis via prodrug conversion, viral protein expression needed to be detected. For this purpose, the used eight cell lines were infected with MeV-SCD at MOI 1 and western blots were performed at 24, 48, 72 and 96 hpi (*Fig. 18*). The defined target proteins were the nucleocapsid-protein (MeV-NP), being expressed in the wildtype measles vaccine virus, and the SCD-protein (MeV-SCD), which is only expressed in our oncolytic measles virus by transgene insertion. Vinculin served as a cellular control. In all eight tested pancreatic cancer cell lines infected with MeV-SCD, viral protein production was detected, which indicates sustainable viral replication. It also became evident that viral protein production correlates with the oncolytic effect: Panc-1 (which was the most susceptible cell line to MeV-

SCD mediated oncolysis without addition of prodrug 5-FC) showed massive viral protein production already 24 hours post infection, whereas Capan-1 (which was the least susceptible cell line to MeV-SCD mediated oncolysis) showed delayed viral protein production, starting 48 hours post infection.

## 3.2. Oncolytic vaccinia virus (GLV-1h94)

### 3.2.1. Oncolytic effect of GLV-1h94 on pancreatic cancer cell lines

To find evidence for a general susceptibility of pancreatic cancer cells to oncolytic virotherapy, a second / different virus needed to be evaluated. The oncolytic vaccinia virus GLV-1h94 uses a different entry mechanism than the measles vaccine virus, but harbors the same prodrug-convertase-system as MeV-SCD.

In order to determine the oncolytic potential of GLV-1h94, the used cell lines were infected with GLV-1h94 for 96 hpi and additional treated with or without the prodrug 5-FC (*Fig. 19a*).

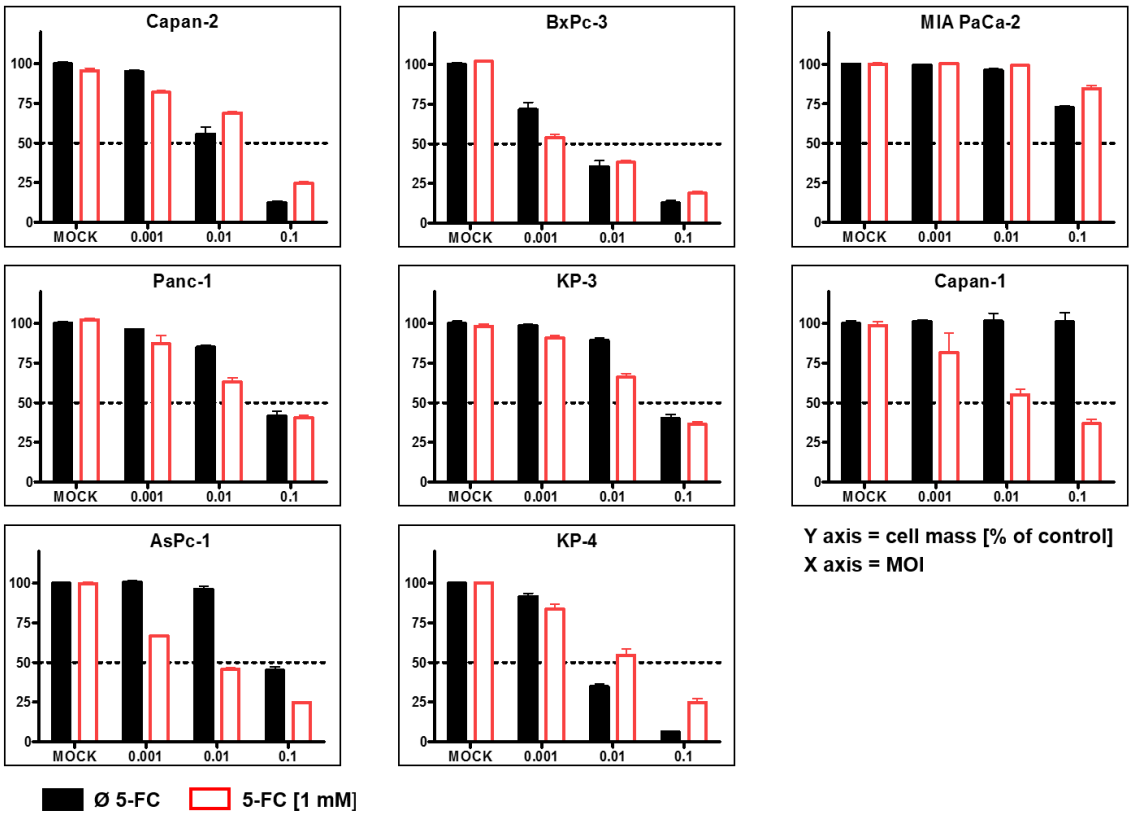


**Fig. 19a: SRB-viability assays 96 hpi withGLV-1h94 with and without addition of prodrug 5-FC.** Viral concentration ranged from MOI 0 (MOCK control), 0.001 to 0.1. The 50 % viability is highlighted as horizontal dotted line.

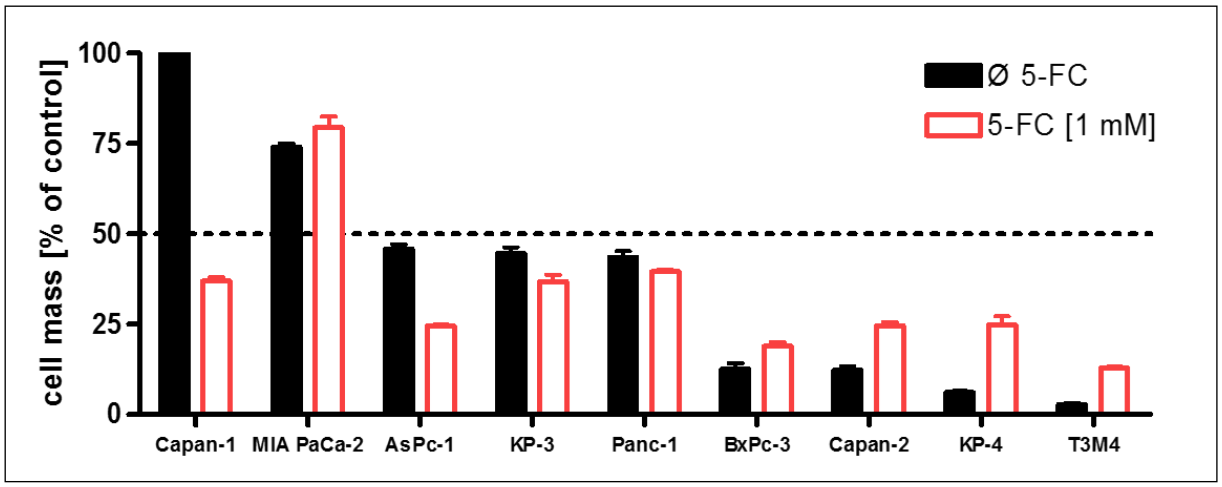


**Fig.19b: Response to GLV-1h94-mediated oncolysis.** All eight cell lines of the used panel of human pancreatic cancer cell lines were infected with GLV-1h94 (at MOI 0.1) and incubated starting from 3 hpi with or without the prodrug 5-FC (1 mM). At 96 hpi, tumor cell viabilities were quantified using the SRB viability assay. Alignment of the eight human pancreatic cancer cell lines from weakest (to the left) to strongest (to the right) oncolytic effect. The dotted horizontal line marks the cutoff being used for definition of primary resistance to GLV-1h94 oncolysis, i.e. more than 50 % viable tumor cells at 96 hpi in comparison to uninfected control tumor cells (MOCK).

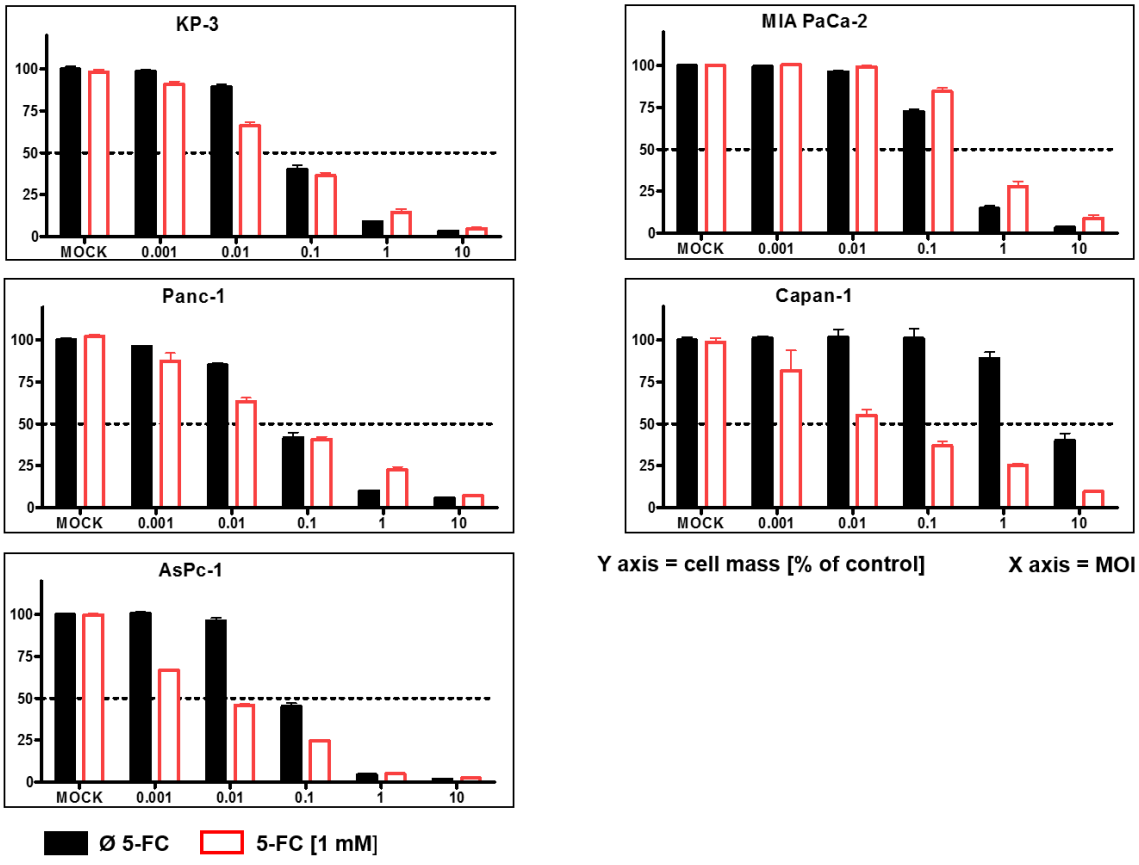


**Fig. 19c: SRB-viability assays 96h post GLV-1h94 infection with and without addition of prodrug 5-FC.** Viral concentration ranges from MOI 0.001 to 10. Primary

resistance to oncolytic effect (horizontal dotted line) is defined by remaining cell mass at MOI 0.1, 96 hours post infection > 50 % of control.

All nine tested human pancreatic cancer cell lines were also susceptible to GLV-1h94-mediated oncolysis, same as for MeV-SCD in a dose / time dependent manner (see *Fig. 19*). Because of the shorter replication cycle of vaccinia virus compared to measles vaccine virus, the cutoff for primary resistance was defined at 50 % viability at MOI 0.1 at 96 hpi (50 % viability at MOI 1 at 96 hpi for MeV-SCD). That definition given, two out of nine pancreatic cancer cell lines were found to be primarily resistant to GLV-1h94-mediated oncolysis. Interestingly, it was again the cell line Capan-1 which showed only minimal susceptibility to this vaccinia virus-mediated virotherapeutic approach. The other resistant cell line to GLV-1h94 treatment was MIA PaCa-2, which was highly susceptible to MeV-SCD-mediated oncolysis.

Furthermore, the addition of the prodrug 5-FC to GLV-1h94-infected cells did not generally enhance GLV-1h94-mediated oncolysis. 5-FC addition only enhanced the oncolytic effect in four but hampered significantly oncolysis in five out of nine cell lines.

Apart from Capan-1, as the most resistant cell line for both used viruses, there was no correlation between the oncolytic effect of MeV-SCD and GLV-1h94. Thus, different outcome patterns can be expected concerning the features of these two distinct virotherapeutic vectors in terms of resistance or susceptibility in human pancreatic cancer cell lines, when used under the same conditions. This is of great interest for the further development of the suicide gene "armed" virotherapy as a novel approach for the treatment of locally advanced or metastatic pancreatic cancer.

## 4. Discussion

Oncolytic virotherapy is a novel and promising approach in cancer treatment. The concept has been preclinically investigated since the 1990s (Russel et al., 2012), with several clinical trials, using different viruses in different tumor entities (Haller et al., 2020) (Li et al., 2020) with the first virotherapeutic compound being FDA- and EMA-approved in 2015. An ideal oncolytic virus is able to selectively target cancer cells while sparing healthy tissue. The virus is replication competent in order to achieve a long-lasting, self-sustaining tumor control. It is easily administered and its genome is open for transgene-insertion in order to enhance the oncolytic activity or to facilitate viral spread within the tumor. Of course, the ideal oncolytic virus is safe to use, having only few, flu-like side effects for the treated patient. MeV-SCD and GLV-1h94 share many of the above listed characteristics of an ideal oncolytic virus and could therefore be considered as novel tools especially for the treatment of locally advanced or metastatic pancreatic cancer.

This thesis work specifically investigated whether the use of two different types of suicide gene-encoding viruses (MeV-SCD and GLV-1h94) would overcome patterns of oncolysis resistance in human pancreatic cancer cell lines. For this purpose, a cell culture panel, consisting of nine different pancreatic cancer cell lines, derived from different origins (primary site and metastasis; male and female original hosts) was defined which should resemble a good spectrum of human pancreatic cancers for this *in vitro* study.

The used cell lines not only differed in growth behavior and morphology, but also in molecular characteristics, in terms of genetic alterations. All examined cell lines, regardless of different distinctions, overexpressed the entry receptor CD46 for MeV-SCD, hence making these cell lines susceptible to infections with MeV-SCD(/-GFP). CD46 expression rates showed a linear correlation with MeV infection rates, thus confirming the concept of the viral entry receptor being essential for viral uptake and spread. We could also prove that infected cells started expression of viral proteins within 24 hpi. This was found to be true also for the inserted suicide transgene. Most importantly, the MeV-mediated oncolysis

also correlated with the primary infection rate, confirming our assumption, that infected cancer cells are unable to clear the infection and thus will be terminated inevitably. The oncolytic effect was found to be time and dose dependent. Only the cell line Capan-1 showed a primary resistance to MeV-mediated oncolysis with still a viability > 50 % at MOI 1 at 96 hpi. This resistance to primary oncolysis was overcome by addition of the prodrug 5-FC, which resulted in enhancement of the oncolytic potential due to an additional "local" 5-FU-mediated cytotoxic effect in almost all examined cell lines.

In 1993 an experiment on the hepatopancreatic uptake and elimination of 5-FU, based on an animal model (mongrel dogs) was performed. Even the intravenous bolus administration of 15 mg/kg 5-FU, which equals the $LD_{50}$ for rabbits, wasn't enough to reach pancreatic fluid concentrations of 5-FU greater than 0.1 mmol/l (Stein et al., 1993). Therefore, it becomes evident that 5-FU concentrations needed to successfully treat pancreatic cancer can't be delivered solely intravenously and that the possibility of locally-induced targeted chemotherapy with 5-FU would provide an immense benefit.

The investigated cell lines were also found to be susceptible to treatment with the suicide gene-encoding vaccinia virus GLV-1h94. Of interest, the oncolytic effect of GLV-1h94 did not correlate with MeV-SCD-mediated oncolysis. The oncolytic effect of GLV-1h94 was, same as for MeV-SCD, dose dependent. Primary resistances of two cell lines could be overcome by a simple dose escalation (usage of higher MOIs). Interestingly, the application of the prodrug 5-FC enhanced the oncolytic activity in only four of the nine examined cell lines.

5-FU is known to compromise viral replication (McCart et al., 2000). *In vitro* experiments with MeV-SCD, analyzing different timepoints and approaches of 5-FC application, already have been performed. Whereas the form of application (pulsed vs. continuous) didn't significantly influence the oncolytic effect, the timepoint was important (Yurttas et al., 2014). Application of 5-FC already at 3 hpi hampered viral spread, probably because the antimetabolite 5-FU is also able to hamper viral replication. This might explain, why the DNA-Virus GLV-1h94 was more affected by 5-FC addition that MeV, an RNA-Virus.

The results of this dissertation are purely based on *in vitro* data, obtained from cell lines that were cultivated for the experiments. As mentioned in the introduction (see chapter 1.1.2), the tumor-environment plays a crucial role in the development and sustainment of pancreatic cancer. There certainly are major differences between a 2-dimensional clonal cell layer in a petri dish or well plate, compared to a 3-dimensional tumor, with all its heterogeneity, stromal tissue and blood supply. A large proportion of PDAC tumor masses consists of non-malignant myofibroblasts and extracellular matrix material (Ryan et al., 2014). Viral cell-to-cell spread and especially the formation of syncytia will most likely be hampered by the dense stromal surroundings of the actual tumor cells. This problem might be addressed in this dissertation by the interesting treatment response of the cell line Capan-1, which was the least susceptible cell line to both MeV-SCD and GLV-1h94 treatment. It was in fact the cell line with the lowest CD46 density on its surface. But as both viruses (MeV-SCD and GLV-1h94) rely on totally different cell entry mechanisms, the common feature might also be due to its specific growth pattern in cell culture. From all nine different cell lines used for the experiments, Capan-1 was the only cell line which did not form a coherent cell layer in the wells / culture flasks during the examined time span of 96 hpi. It grew as cell nests, each containing only few cells with large gaps between the nests. Since MeV-SCD not only spreads via cell lysis and release of new infectious viral particles, but also by cell-to-cell fusion and formation of giant-cell multinucleated syncytia, and vaccinia virus also spreads by cell-to-cell contact, passing intracellular enveloped viruses (IEV) from an infected to a neighbouring cell, the incoherent growth pattern of Capan-1 probably physically hampers this form of viral spread. Some attempts which specifically target this problem have already been performed by establishing *in vitro* 3-dimensional tumor cell cultures, some of which have recently been analyzed in the context of virotherapeutic research (Kloker et al., 2018) and by forming patient-derived pancreatic tumor organoids in order to predict response to (adenovirus-mediated) oncolytic virotherapy (Raimondi et al., 2020). Another interesting approach is the development of a virtual / mathematical model of how oncolytic viruses spread

through pancreatic cancer, which has recently successfully been developed (Chen et al., 2020).

From a different therapeutic perspective, the tumor surrounding doesn't necessarily need to be seen as a barrier for oncolytic virotherapy. In fact, many therapeutic compounds, like cytotoxic chemotherapy, are already naturally hampered by the tumor microenvironment. In this context, oncolytic virotherapy could be considered as an immune-modulator in a combination therapy (Tassone et al., 2020). This therapeutic approach has already led to some clinical trials with combination therapies of OV and conventional chemotherapy, (see chapter 1.2.5), but the results have been disappointing so far.

Apart from the disregard of stromal tissue in this cell-culture-based study, another limitation that needs to be addressed would be the missing inclusion of an adaptive immune system. In order to spread within a tumor and work to its full potential (as displayed in most cell-culture-based models), oncolytic viruses have to reach the tumor site. Most clinical trials examining PDAC treatment with oncolytic viruses eluded this problem by direct intratumoral injection (Haller et al., 2020). Still, if the virus starts to infect the tumor (which it is supposed to do), the adaptive immune system will eventually get triggered, interact and try to neutralize the virus. Due to the cell culture approach of this thesis, this aspect could not be examined in this study and needs further investigations.

In summary, this dissertation provides evidence for the efficacy of MeV-SCD and GLV-1h94 as therapeutic agents in combination with 5-FC for the treatment of pancreatic cancer.

Perspectives

At the time, one can say that there are two different approaches of how oncolytic virotherapy might contribute to clinical oncology in the future: improving virus

mediated oncolysis vs. utilizing the virus as immunomodulatory co-factor in a combination therapy with lesser focus on the virus-induced oncolysis.

By genetic alteration / modification, the possibilities of “sharpening the weapons” of oncolytic viruses are sheer endless. Different strains of numerous types of viruses are yet to be evaluated in preclinical or even clinical trials, aiming to establish oncolytic viruses as therapeutic add-on or even alternative to conventional cytotoxic chemotherapies (Lin et al., 2023).
For example, a recombinant version of the quite virulent vesicular stomatitis virus (VSV), was recently genetically modified to use the MeV-entry receptor CD46. This aims to improve the safety of VSV derived virotherapy by limiting side effects by targeting it more precisely at CD46-expressing malignant tumors. Interestingly, this concept worked fine with hepato-biliary and pancreatic cancer cells *in vitro*, whereas the recombinant VSV was only able to control the hepato-biliary tumor cells, but not the pancreatic cancer cells in a mouse xenograft model (Nagalo et al., 2020).
Another, much-noticed example for the therapeutic benefit of OV treatment has very recently been published, when 37 patients with triple-negative breast cancer have been treated with the HSV-1 derived oncolytic virus T-VEC in the neoadjuvant setting. In this study, all patients were treated with the standard-of-care chemotherapy regimen with paclitaxel, doxorubicin, cyclophosphamide and pegfilgrastim in combination with (up to) five intratumoral injections of T-VEC. 65 % of the treated patients had a clinically significant response, compared to a (literature based) 44 % response rate for chemotherapy only (Soliman H et al., 2023).

Virotherapy combined with immunotherapy

One major disadvantage of *in vitro* models will always be the missing interaction of the OV with a fully intact, human host immune system, which has to be considered when studying a replication competent virus as a therapeutic agent. The fact that the only FDA- / EMA-approved virotherapeutic T-VEC showed clinical efficiency / benefit for the treatment of malignant melanoma, might

certainly be due to host-immune-system interactions. Melanomas are known for their high immunogenicity in comparison to other tumor entities, meaning that the host immune system is more likely to detect and fight melanoma cells. This has led to the emerging field of cancer immunotherapy, e.g. usage of immune checkpoint inhibition, which successfully aims to achieve tumor control by modulating the patient's immune system against the tumor (Pardoll DM, 2012). For the discovery of the principle of checkpoint inhibition, *James P. Allison* and *Tasuku Honjo* were awarded with the *Nobel prize in Physiology or Medicine* in 2018.

There is evidence, that oncolytic virotherapy can contribute to an immune checkpoint blockade targeted therapy (Harrington et al., 2019) (Ripp et al., 2022). Lymphocytic infiltration of tumors seems to be associated with improved survival, thought to be due to increased immunogenicity by tumor inflammation (Gibney et al., 2016). Oncolytic viruses could be utilized to induce such inflammation, thus enhance the host immune response against the tumor, which could work synergistic with an immune checkpoint inhibition (Melcher et al., 2021). Preclinical experiments with an oncolytic Newcastle disease virus (NDV) showed very interesting results, as the intratumoral injection of the virus had led to migration of tumor-specific $CD4^+$ and $CD8^+$ to distant tumor manifestations. The combination of the NDV intratumoral treatment with systemic application of a checkpoint-inhibitor could even increase the therapeutic response (Zamarin et al., 2014). Another preclinical study evaluated the oncolytic potential of a genetically engineered orthopoxvirus, armed with a sodium iodine symporter and an anti-PD-L1-antibody in a PDAC peritoneal carcinosis mouse model with promising results (Woo et al., 2020). A recently published study utilized a mismatch repair-deficient colorectal carcinoma mouse model for the combination of immune checkpoint inhibition, low-dose chemotherapy and oncolytic HSV-1 mediated virotherapy (El-Sayes et al., 2022). The combination therapy induced $CD4^+$ and $CD8^+$ lymphocyte as well as dendritic cell infiltration into the tumor.
First human trials have also been attempted. An uncontrolled, phase Ib clinical trial (n=21), investigating a combination therapy of T-VEC and pembrolizumab for the treatment of melanoma showed an overall response rate of 66 % with a

complete response rate of 33 % (Ribas et al., 2017). Although, the enrollment criteria didn't state that directly, 11 out of the 21 patients (52 %) had already been treated prior to the virotherapeutic treatment approach.
Another recent multicenter, parallel-cohort, phase Ib trial used T-VEC in combination with the anti-PD-L1 antibody atezolizumab for the treatment of triple-negative breast cancer (n=10) and colorectal carcinoma (n=24) which had already developed liver metastasis. T-VEC was administered via intratumoral injection. Of all patients treated in this trial, only one patient in the breast cancer cohort had a partial response and none in the colorectal cancer cohort (Hecht JR, 2023). Tumoral PD1-expression was not examined in this trial, but still the limited antitumor activity clearly indicates that further investigation in this field is needed.

One can state, that the future of oncolytic virotherapy will most likely be in the field of cancer immunotherapy. There is enough evidence which supports the idea that virotherapy may contribute to a better response to immune checkpoint inhibition. Although it is an emerging field, to date there are only few tumor entities which do respond primarily well to cancer immunotherapy. Pancreatic cancer remains a dismal prognosis to date. Although cancer immunotherapy can be seen as revolutionary, only a very small proportion of PDAC (< 2 %) show clinical features which may lead to immune checkpoint susceptibility (Ahmad-Nielsen et al., 2020).
Virotherapy may find its clinical standing as an immune modulator, changing the tumors microenvironment and making it more susceptible to immunotherapy.

**Summary**

Pancreatic cancer is one of the leading causes for cancer related death in Germany. Many patients already present with a locally advanced or even metastatic state of this dismal disease. Therapeutic options at this stage are limited and the benefit in terms of prolonged overall survival is still underwhelming.

Oncolytic virotherapy is a relatively novel therapeutic approach for the treatment of extensive disease cancer. The oncolytic measles vaccine virus MeV-SCD as well as the oncolytic vaccinia virus GLV-1h94 encode for a clinically useable prodrug convertase system, enabling infected cells to convert nontoxic 5-fluorocytosine into the well-known chemotherapeutic compound 5-fluorouracil intracellularly. Both viruses have been shown to exert great oncolytic activity against a variety of different cancer cell lines.

This dissertation aimed to find proof if the two different suicide gene-encoding oncolytic viral vectors MeV-SCD and GLV-1h94 were able to infect and lyse pancreatic cancer cells in an in-vitro model. This was done by FACS-analysis, fluorescence microscopy, cell viability assays and western blotting.

All eight pancreatic cancer cell lines were susceptible to the OV treatment in a dose / time dependent manner. Primary resistance could be overcome by dose / time escalation and activation of the prodrug-convertase system by additional treatment with 5-FC. With both viruses being replication competent therapeutic agents, their mechanism of intratumoral spreading and oncolysis differed a lot, leading to completely different outcome patterns.

The finding, that both MeV-SCD and GLV-1h94 were able to infect pancreatic cancer cells, knowing that tumor infection can change the tumor microenvironment, contributing to a better immune response raises hope, that one day oncolytic virotherapy might function as an immunotherapy-enabler.

Of course, this needs further evaluation / optimization, as in the future there may be a variety of different oncolytic viruses of different viral strains encoding for different transgenes to choose from.

## References


Andtbacka RHI, Collichio F, Harrington KJ, Middleton MR, Downey G, Öhrling K, Kaufman HL. Final analyses of OPTiM: a randomized phase III trial of talimogene laherparepvec versus granulocyte-macrophage colony-stimulating factor in unresectable stage III-IV melanoma. J Immunother Cancer. 2019 Jun 6;7(1):145. doi: 10.1186/s40425-019-0623-z. PMID: 31171039; PMCID: PMC6554874.

Antoine G, Scheiflinger F, Dorner F, Falkner FG. The complete genomic sequence of the modified vaccinia Ankara strain: comparison with other orthopoxviruses. Virology. 1998 May 10;244(2):365-96. doi: 10.1006/viro.1998.9123. Erratum in: Virology. 2006 Jul 5;350(2):501-2. PMID: 9601507.

Baxby D. The origins of vaccinia virus. J Infect Dis. 1977 Sep;136(3):453-5. doi: 10.1093/infdis/136.3.453. PMID: 198484.

Berchtold S, Beil J, Raff C, Smirnow I, Schell M, D'Alvise J, Gross S, Lauer UM. Assessing and Overcoming Resistance Phenomena against a Genetically Modified Vaccinia Virus in Selected Cancer Cell Lines. Int J Mol Sci. 2020 Oct 15;21(20):7618. doi: 10.3390/ijms21207618. PMID: 33076270; PMCID: PMC7589280.

Bluming AZ, Ziegler JL. Regression of Burkitt's lymphoma in association with measles infection. Lancet. 1971 Jul 10;2(7715):105-6. doi: 10.1016/s0140-6736(71)92086-1. PMID: 4103972.

Broyles SS. Vaccinia virus transcription. J Gen Virol. 2003 Sep;84(Pt 9):2293-2303. doi: 10.1099/vir.0.18942-0. PMID: 12917449.

Bossow S, Grossardt C, Temme A, Leber MF, Sawall S, Rieber EP, Cattaneo R, von Kalle C, Ungerechts G. Armed and targeted measles virus for chemovirotherapy of pancreatic cancer. Cancer Gene Ther. 2011 Aug;18(8):598-608. doi: 10.1038/cgt.2011.30. Epub 2011 Jun 24. PMID: 21701532; PMCID: PMC3914720.

Burris HA 3rd, Moore MJ, Andersen J, Green MR, Rothenberg ML, Modiano MR, Cripps MC, Portenoy RK, Storniolo AM, Tarassoff P, Nelson R, Dorr FA, Stephens CD, Von Hoff DD. Improvements in survival and clinical benefit with gemcitabine as first-line therapy for patients with advanced pancreas cancer: a randomized trial. J Clin Oncol. 1997 Jun;15(6):2403-13. doi: 10.1200/JCO.1997.15.6.2403. PMID: 9196156.

Carter GC, Rodger G, Murphy BJ, Law M, Krauss O, Hollinshead M, Smith GL. Vaccinia virus cores are transported on microtubules. J Gen Virol. 2003 Sep;84(Pt 9):2443-2458. doi: 10.1099/vir.0.19271-0. PMID: 12917466.

Chen J, Weihs D, Vermolen FJ. A Cellular Automata Model of Oncolytic Virotherapy in Pancreatic Cancer. Bull Math Biol. 2020 Jul 31;82(8):103. doi: 10.1007/s11538-020-00780-5. PMID: 32737595; PMCID: PMC7395005.

Chen N, Zhang Q, Yu YA, Stritzker J, Brader P, Schirbel A, Samnick S, Serganova I, Blasberg R, Fong Y, Szalay AA. A novel recombinant vaccinia virus expressing the human norepinephrine transporter retains oncolytic potential and facilitates deep-tissue imaging. Mol Med. 2009 May-Jun;15(5-6):144-51. doi: 10.2119/molmed.2009.00014. Epub 2009 Feb 25. PMID: 19287510; PMCID: PMC2654849.

Combredet C, Labrousse V, Mollet L, Lorin C, Delebecque F, Hurtrel B, McClure H, Feinberg MB, Brahic M, Tangy F. A molecularly cloned Schwarz strain of measles virus vaccine induces strong immune responses in macaques and transgenic mice. J Virol. 2003 Nov;77(21):11546-54. doi: 10.1128/jvi.77.21.11546-11554.2003. PMID: 14557640; PMCID: PMC229349.

Conroy T, Desseigne F, Ychou M, Bouché O, Guimbaud R, Bécouarn Y, Adenis A, Raoul JL, Gourgou-Bourgade S, de la Fouchardière C, Bennouna J, Bachet JB, Khemissa-Akouz F, Péré-Vergé D, Delbaldo C, Assenat E, Chauffert B, Michel P, Montoto-Grillot C, Ducreux M; Groupe Tumeurs Digestives of Unicancer; PRODIGE Intergroup. FOLFIRINOX versus gemcitabine for metastatic pancreatic cancer. N Engl J Med. 2011 May 12;364(19):1817-25. doi: 10.1056/NEJMoa1011923. PMID: 21561347.

Conroy T, Hammel P, Hebbar M, Ben Abdelghani M, Wei AC, Raoul JL, Choné L, Francois E, Artru P, Biagi JJ, Lecomte T, Assenat E, Faroux R, Ychou M, Volet J, Sauvanet A, Breysacher G, Di Fiore F, Cripps C, Kavan P, Texereau P, Bouhier-Leporrier K, Khemissa-Akouz F, Legoux JL, Juzyna B, Gourgou S, O'Callaghan CJ, Jouffroy-Zeller C, Rat P, Malka D, Castan F, Bachet JB; Canadian Cancer Trials Group and the Unicancer-GI–PRODIGE Group. FOLFIRINOX or Gemcitabine as Adjuvant Therapy for Pancreatic Cancer. N Engl J Med. 2018 Dec 20;379(25):2395-2406. doi: 10.1056/NEJMoa1809775. PMID: 30575490.

Dörig RE, Marcil A, Chopra A, Richardson CD. The human CD46 molecule is a receptor for measles virus (Edmonston strain). Cell. 1993 Oct 22;75(2):295-305. doi: 10.1016/0092-8674(93)80071-l. PMID: 8402913.

Downward J. Targeting RAS signalling pathways in cancer therapy. Nat Rev Cancer. 2003 Jan;3(1):11-22. doi: 10.1038/nrc969. PMID: 12509763.

El-Sayes N, Vito A, Salem O, Workenhe ST, Wan Y, Mossman K. A Combination of Chemotherapy and Oncolytic Virotherapy Sensitizes Colorectal Adenocarcinoma to Immune Checkpoint Inhibitors in a cDC1-Dependent Manner. Int J Mol Sci. 2022 Feb 3;23(3):1754. doi: 10.3390/ijms23031754. PMID: 35163675; PMCID: PMC8915181.

Geessien Kroon E, Santos Abrahão J, de Souza Trindade G, Pereira Oliveira G, Moreira Franco Luiz AP, Barbosa Costa G, Teixeira Lima M, Silva Calixto R, de Oliveira DB, Drumond BP. Natural Vaccinia Virus Infection: Diagnosis, Isolation, and Characterization. Curr Protoc Microbiol. 2016 Aug 12;42:14A.5.1-14A.5.43. doi: 10.1002/cpmc.13. PMID: 27517335.

Geller A, Yan J. The Role of Membrane Bound Complement Regulatory Proteins in Tumor Development and Cancer Immunotherapy. Front Immunol. 2019 May 21;10:1074. doi: 10.3389/fimmu.2019.01074. PMID: 31164885; PMCID: PMC6536589.

Gibney GT, Weiner LM, Atkins MB. Predictive biomarkers for checkpoint inhibitor-based immunotherapy. Lancet Oncol. 2016 Dec;17(12):e542-e551. doi: 10.1016/S1470-2045(16)30406-5. PMID: 27924752; PMCID: PMC5702534.

Graepler F, Lemken ML, Wybranietz WA, Schmidt U, Smirnow I, Gross CD, Spiegel M, Schenk A, Graf H, Lauer UA, Vonthein R, Gregor M, Armeanu S, Bitzer M, Lauer UM. Bifunctional chimeric SuperCD suicide gene -YCD: YUPRT fusion is highly effective in a rat hepatoma model. World J Gastroenterol. 2005 Nov 28;11(44):6910-9. doi: 10.3748/wjg.v11.i44.6910. PMID: 16437592; PMCID: PMC4717030.

Guo ZS, Lu B, Guo Z, Giehl E, Feist M, Dai E, Liu W, Storkus WJ, He Y, Liu Z, Bartlett DL. Vaccinia virus-mediated cancer immunotherapy: cancer vaccines and oncolytics. J Immunother Cancer. 2019 Jan 9;7(1):6. doi: 10.1186/s40425-018-0495-7. PMID: 30626434; PMCID: PMC6325819.

Hajda J, Lehmann M, Krebs O, Kieser M, Geletneky K, Jäger D, Dahm M, Huber B, Schöning T, Sedlaczek O, Stenzinger A, Halama N, Daniel V, Leuchs B, Angelova A, Rommelaere J, Engeland CE, Springfeld C, Ungerechts G. A non-controlled, single arm, open label, phase II study of intravenous and intratumoral administration of ParvOryx in patients with metastatic, inoperable pancreatic cancer: ParvOryx02 protocol. BMC Cancer. 2017 Aug 29;17(1):576. doi: 10.1186/s12885-017-3604-y. PMID: 28851316; PMCID: PMC5574242.

Haller SD, Monaco ML, Essani K. The Present Status of Immuno-Oncolytic Viruses in the Treatment of Pancreatic Cancer. Viruses. 2020 Nov 17;12(11):1318. doi: 10.3390/v12111318. PMID: 33213031; PMCID: PMC7698570.

Harrington K, Freeman DJ, Kelly B, Harper J, Soria JC. Optimizing oncolytic virotherapy in cancer treatment. Nat Rev Drug Discov. 2019 Sep;18(9):689-706. doi: 10.1038/s41573-019-0029-0. Epub 2019 Jul 10. PMID: 31292532.

Hartkopf AD, Bossow S, Lampe J, Zimmermann M, Taran FA, Wallwiener D, Fehm T, Bitzer M, Lauer UM. Enhanced killing of ovarian carcinoma using oncolytic measles vaccine virus armed with a yeast cytosine deaminase and uracil phosphoribosyltransferase. Gynecol Oncol. 2013 Aug;130(2):362-8. doi: 10.1016/j.ygyno.2013.05.004. Epub 2013 May 12. PMID: 23676551.

Hecht JR, Raman SS, Chan A, Kalinsky K, Baurain JF, Jimenez MM, Garcia MM, Berger MD, Lauer UM, Khattak A, Carrato A, Zhang Y, Liu K, Cha E, Keegan A, Bhatta S, Strassburg CP, Roohullah A. Phase Ib study of talimogene laherparepvec in combination with atezolizumab in patients with triple negative breast cancer and colorectal cancer with liver metastases. ESMO Open. 2023 Apr;8(2):100884. doi: 10.1016/j.esmoop.2023.100884. Epub 2023 Feb 28. PMID: 36863095.

Hecht JR, Bedford R, Abbruzzese JL, Lahoti S, Reid TR, Soetikno RM, Kirn DH, Freeman SM. A phase I/II trial of intratumoral endoscopic ultrasound injection of ONYX-015 with intravenous gemcitabine in unresectable pancreatic carcinoma. Clin Cancer Res. 2003 Feb;9(2):555-61. PMID: 12576418.

Hidalgo M. Pancreatic cancer. N Engl J Med. 2010 Apr 29;362(17):1605-17. doi: 10.1056/NEJMra0901557. Erratum in: N Engl J Med. 2010 Jul 15;363(3):298. PMID: 20427809.

Hruban RH, Goggins M, Parsons J, Kern SE. Progression model for pancreatic cancer. Clin Cancer Res. 2000 Aug;6(8):2969-72. PMID: 10955772.

Liggett WH Jr, Sidransky D. Role of the p16 tumor suppressor gene in cancer. J Clin Oncol. 1998 Mar;16(3):1197-206. doi: 10.1200/JCO.1998.16.3.1197. PMID: 9508208.

Kamisawa T, Wood LD, Itoi T, Takaori K. Pancreatic cancer. Lancet. 2016 Jul 2;388(10039):73-85. doi: 10.1016/S0140-6736(16)00141-0. Epub 2016 Jan 30. PMID: 26830752.

Kassenärztliche Bundesvereinigung [homepage]. Available from https://www.kbv.de/html/15147.php, accessed on 24/03/2021

Kastenhuber ER, Lowe SW. Putting p53 in Context. Cell. 2017 Sep 7;170(6):1062-1078. doi: 10.1016/j.cell.2017.08.028. PMID: 28886379; PMCID: PMC5743327.

Kelly KJ, Wong J, Gönen M, Allen P, Brennan M, Coit D, Fong Y. Human Trial of a Genetically Modified Herpes Simplex Virus for Rapid Detection of Positive Peritoneal Cytology in the Staging of Pancreatic Cancer. EBioMedicine. 2016 May;7:94-9. doi: 10.1016/j.ebiom.2016.03.043. Epub 2016 Apr 2. PMID: 27322463; PMCID: PMC4909379.

Kim JY, Hong SM. Precursor Lesions of Pancreatic Cancer. Oncol Res Treat. 2018;41(10):603-610. doi: 10.1159/000493554. Epub 2018 Sep 28. PMID: 30269131.

Kloker LD, Yurttas C, Lauer UM. Three-dimensional tumor cell cultures employed in virotherapy research. Oncolytic Virother. 2018 Sep 5;7:79-93. doi: 10.2147/OV.S165479. PMID: 30234074; PMCID: PMC6130269.

Laemmli UK. Cleavage of structural proteins during the assembly of the head of bacteriophage T4. Nature. 1970 Aug 15;227(5259):680-5. doi: 10.1038/227680a0. PMID: 5432063.

Laksono BM, de Vries RD, McQuaid S, Duprex WP, de Swart RL. Measles Virus Host Invasion and Pathogenesis. Viruses. 2016 Jul 28;8(8):210. doi: 10.3390/v8080210. PMID: 27483301; PMCID: PMC4997572.

Lampe J, Bossow S, Weiland T, Smirnow I, Lehmann R, Neubert W, Bitzer M, Lauer UM. An armed oncolytic measles vaccine virus eliminates human hepatoma cells independently of apoptosis. Gene Ther. 2013 Nov;20(11):1033-41. doi: 10.1038/gt.2013.28. Epub 2013 May 30. PMID: 23719065.

Lange S, Lampe J, Bossow S, Zimmermann M, Neubert W, Bitzer M, Lauer UM. A novel armed oncolytic measles vaccine virus for the treatment of cholangiocarcinoma. Hum Gene Ther. 2013 May;24(5):554-64. doi: 10.1089/hum.2012.136. PMID: 23550539; PMCID: PMC3655633.

Lauer UM, Beil J. Oncolytic viruses: challenges and considerations in an evolving clinical landscape. Future Oncol. 2022 Jul 12. doi: 10.2217/fon-2022-0440. Epub ahead of print. PMID: 35818970.

Lawler SE, Speranza MC, Cho CF, Chiocca EA. Oncolytic Viruses in Cancer Treatment: A Review. JAMA Oncol. 2017 Jun 1;3(6):841-849. doi: 10.1001/jamaoncol.2016.2064. PMID: 27441411.

Lee HS, Park SW. Systemic Chemotherapy in Advanced Pancreatic Cancer. Gut Liver. 2016 May 23;10(3):340-7. doi: 10.5009/gnl15465. PMID: 27114434; PMCID: PMC4849685.

Lee JC, Shin DW, Park H, Kim J, Youn Y, Kim JH, Kim J, Hwang JH. Tolerability and safety of EUS-injected adenovirus-mediated double-suicide gene therapy with chemotherapy in locally advanced pancreatic cancer: a phase 1 trial. Gastrointest

Endosc. 2020 Nov;92(5):1044-1052.e1. doi: 10.1016/j.gie.2020.02.012. Epub 2020 Feb 19. PMID: 32084409.

Lemos de Matos A, Franco LS, McFadden G. Oncolytic Viruses and the Immune System: The Dynamic Duo. Mol Ther Methods Clin Dev. 2020 Jan 15;17:349-358. doi: 10.1016/j.omtm.2020.01.001. PMID: 32071927; PMCID: PMC7015832.

Li Y, Shen Y, Zhao R, Samudio I, Jia W, Bai X, Liang T. Oncolytic virotherapy in hepato-bilio-pancreatic cancer: The key to breaking the log jam? Cancer Med. 2020 May;9(9):2943-2959. doi: 10.1002/cam4.2949. Epub 2020 Mar 4. PMID: 32130786; PMCID: PMC7196045.

Lin D, Shen Y, Liang T. Oncolytic virotherapy: basic principles, recent advances and future directions. Signal Transduct Target Ther. 2023 Apr 11;8(1):156. doi: 10.1038/s41392-023-01407-6. PMID: 37041165; PMCID: PMC10090134.

Liszewski MK, Post TW, Atkinson JP. Membrane cofactor protein (MCP or CD46): newest member of the regulators of complement activation gene cluster. Annu Rev Immunol. 1991;9:431-55. doi: 10.1146/annurev.iy.09.040191.002243. PMID: 1910685.

Ludlow M, McQuaid S, Milner D, de Swart RL, Duprex WP. Pathological consequences of systemic measles virus infection. J Pathol. 2015 Jan;235(2):253-65. doi: 10.1002/path.4457. PMID: 25294240.

Mahalingam D, Goel S, Aparo S, Patel Arora S, Noronha N, Tran H, Chakrabarty R, Selvaggi G, Gutierrez A, Coffey M, Nawrocki ST, Nuovo G, Mita MM. A Phase II Study of Pelareorep (REOLYSIN®) in Combination with Gemcitabine for Patients with Advanced Pancreatic Adenocarcinoma. Cancers (Basel). 2018 May 25;10(6):160. doi: 10.3390/cancers10060160. PMID: 29799479; PMCID: PMC6025223.

Mahaseth H, Brutcher E, Kauh J, Hawk N, Kim S, Chen Z, Kooby DA, Maithel SK, Landry J, El-Rayes BF. Modified FOLFIRINOX regimen with improved safety and maintained efficacy in pancreatic adenocarcinoma. Pancreas. 2013 Nov;42(8):1311-5. doi: 10.1097/MPA.0b013e31829e2006. PMID: 24152956.

Maurer S, Salih HR, Smirnow I, Lauer UM, Berchtold S. Suicide gene-armed measles vaccine virus for the treatment of AML. Int J Oncol. 2019 Aug;55(2):347-358. doi: 10.3892/ijo.2019.4835. Epub 2019 Jul 2. PMID: 31268165; PMCID: PMC6615925.

McCart JA, Puhlmann M, Lee J, Hu Y, Libutti SK, Alexander HR, Bartlett DL. Complex interactions between the replicating oncolytic effect and the enzyme/prodrug effect of vaccinia-mediated tumor regression. Gene Ther. 2000 Jul;7(14):1217-23. doi: 10.1038/sj.gt.3301237. PMID: 10918490.

Melcher A, Harrington K, Vile R. Oncolytic virotherapy as immunotherapy. Science. 2021 Dec 10;374(6573):1325-1326. doi: 10.1126/science.abk3436. Epub 2021 Dec 9. PMID: 34882456; PMCID: PMC8961675.

Mercer J, Helenius A. Virus entry by macropinocytosis. Nat Cell Biol. 2009 May;11(5):510-20. doi: 10.1038/ncb0509-510. PMID: 19404330.

Moss B. Poxvirus cell entry: how many proteins does it take? Viruses. 2012 May;4(5):688-707. doi: 10.3390/v4050688. Epub 2012 Apr 27. PMID: 22754644; PMCID: PMC3386626.

Moss WJ. Measles. Lancet. 2017 Dec 2;390(10111):2490-2502. doi: 10.1016/S0140-6736(17)31463-0. Epub 2017 Jun 30. PMID: 28673424.

Mühlebach MD, Mateo M, Sinn PL, Prüfer S, Uhlig KM, Leonard VH, Navaratnarajah CK, Frenzke M, Wong XX, Sawatsky B, Ramachandran S, McCray PB Jr, Cichutek K, von Messling V, Lopez M, Cattaneo R. Adherens junction protein nectin-4 is the epithelial receptor for measles virus. Nature. 2011 Nov 2;480(7378):530-3. doi: 10.1038/nature10639. PMID: 22048310; PMCID: PMC3245798.

Nagalo BM, Breton CA, Zhou Y, Arora M, Bogenberger JM, Barro O, Steele MB, Jenks NJ, Baker AT, Duda DG, Roberts LR, Russell SJ, Peng KW, Borad MJ. Oncolytic Virus with Attributes of Vesicular Stomatitis Virus and Measles Virus in Hepatobiliary and Pancreatic Cancers. Mol Ther Oncolytics. 2020 Sep 25;18:546-555. doi: 10.1016/j.omto.2020.08.007. Epub 2020 Aug 19. PMID: 32839735; PMCID: PMC7437509.

Nakao A, Kasuya H, Sahin TT, Nomura N, Kanzaki A, Misawa M, Shirota T, Yamada S, Fujii T, Sugimoto H, Shikano T, Nomoto S, Takeda S, Kodera Y, Nishiyama Y. A phase I dose-escalation clinical trial of intraoperative direct intratumoral injection of HF10 oncolytic virus in non-resectable patients with advanced pancreatic cancer. Cancer Gene Ther. 2011 Mar;18(3):167-75. doi: 10.1038/cgt.2010.65. Epub 2010 Nov 19. PMID: 21102422.

NIH U.S. National Library of Medicine [homepage], accessible from https://clinicaltrials.gov/ct2/home, accessed on 25/03/2021

Noonan AM, Farren MR, Geyer SM, Huang Y, Tahiri S, Ahn D, Mikhail S, Ciombor KK, Pant S, Aparo S, Sexton J, Marshall JL, Mace TA, Wu CS, El-Rayes B, Timmers CD, Zwiebel J, Lesinski GB, Villalona-Calero MA, Bekaii-Saab TS. Randomized Phase 2 Trial of the Oncolytic Virus Pelareorep (Reolysin) in Upfront Treatment of Metastatic Pancreatic Adenocarcinoma. Mol Ther. 2016 Jun;24(6):1150-1158. doi: 10.1038/mt.2016.66. Epub 2016 Apr 4. PMID: 27039845; PMCID: PMC4923331.

Oliveira JS, Figueiredo PO, Costa GB, Assis FL, Drumond BP, da Fonseca FG, Nogueira ML, Kroon EG, Trindade GS. Vaccinia Virus Natural Infections in Brazil: The Good, the Bad, and the Ugly. Viruses. 2017 Nov 15;9(11):340. doi: 10.3390/v9110340. PMID: 29140260; PMCID: PMC5707547.

Pardoll DM. The blockade of immune checkpoints in cancer immunotherapy. Nat Rev Cancer. 2012 Mar 22;12(4):252-64. doi: 10.1038/nrc3239. PMID: 22437870; PMCID: PMC4856023.

Raimondi G, Mato-Berciano A, Pascual-Sabater S, Rovira-Rigau M, Cuatrecasas M, Fondevila C, Sánchez-Cabús S, Begthel H, Boj SF, Clevers H, Fillat C. Patient-derived pancreatic tumour organoids identify therapeutic responses to oncolytic adenoviruses. EBioMedicine. 2020 Jun;56:102786. doi: 10.1016/j.ebiom.2020.102786. Epub 2020 May 24. PMID: 32460166; PMCID: PMC7251378.

Ribas A, Dummer R, Puzanov I, VanderWalde A, Andtbacka RHI, Michielin O, Olszanski AJ, Malvehy J, Cebon J, Fernandez E, Kirkwood JM, Gajewski TF, Chen L, Gorski KS, Anderson AA, Diede SJ, Lassman ME, Gansert J, Hodi FS, Long GV. Oncolytic Virotherapy Promotes Intratumoral T Cell Infiltration and Improves Anti-PD-1 Immunotherapy. Cell. 2017 Sep 7;170(6):1109-1119.e10. doi: 10.1016/j.cell.2017.08.027. Erratum in: Cell. 2018 Aug 9;174(4):1031-1032. PMID: 28886381.

Ripp J, Hentzen S, Saeed A. Oncolytic Viruses as an Adjunct to Immune Checkpoint Inhibition. Front Biosci (Landmark Ed). 2022 May 10;27(5):151. doi: 10.31083/j.fbl2705151. PMID: 35638418.

Robert Koch Institut, „Krebs in Deutschland 2005/2006“, „Krebs in Deutschland 2011/2012“, „Krebs in Deutschland 2015/2016“

Russell SJ, Peng KW, Bell JC. Oncolytic virotherapy. Nat Biotechnol. 2012 Jul 10;30(7):658-70. doi: 10.1038/nbt.2287. PMID: 22781695; PMCID: PMC3888062.

Ryan DP, Hong TS, Bardeesy N. Pancreatic adenocarcinoma. N Engl J Med. 2014 Nov 27;371(22):2140-1. doi: 10.1056/NEJMc1412266. PMID: 25427123.

Salzman NP. The rate of formation of vaccinia deoxyribonucleic acid and vaccinia virus. Virology. 1960 Jan;10:150-2. doi: 10.1016/0042-6822(60)90015-5. PMID: 14441184.

Schmidt FI, Bleck CK, Mercer J. Poxvirus host cell entry. Curr Opin Virol. 2012 Feb;2(1):20-7. doi: 10.1016/j.coviro.2011.11.007. Epub 2011 Dec 27. PMID: 22440962.

Sener SF, Fremgen A, Menck HR, Winchester DP. Pancreatic cancer: a report of treatment and survival trends for 100,313 patients diagnosed from 1985-1995, using the National Cancer Database. J Am Coll Surg. 1999 Jul;189(1):1-7. doi: 10.1016/s1072-7515(99)00075-7. PMID: 10401733.

Siegel R, Naishadham D, Jemal A. Cancer statistics, 2013. CA Cancer J Clin. 2013 Jan;63(1):11-30. doi: 10.3322/caac.21166. Epub 2013 Jan 17. PMID: 23335087.

Skehan P, Storeng R, Scudiero D, Monks A, McMahon J, Vistica D, Warren JT, Bokesch H, Kenney S, Boyd MR. New colorimetric cytotoxicity assay for anticancer-drug screening. J Natl Cancer Inst. 1990 Jul 4;82(13):1107-12. doi: 10.1093/jnci/82.13.1107. PMID: 2359136.

Soliman H, Hogue D, Han H, Mooney B, Costa R, Lee MC, Niell B, Williams A, Chau A, Falcon S, Soyano A, Armaghani A, Khakpour N, Weinfurtner RJ, Hoover S, Kiluk J, Laronga C, Rosa M, Khong H, Czerniecki B. Oncolytic T-VEC virotherapy plus neoadjuvant chemotherapy in nonmetastatic triple-negative breast cancer: a phase 2 trial. Nat Med. 2023 Feb;29(2):450-457. doi: 10.1038/s41591-023-02210-0. Epub 2023 Feb 9. Erratum in: Nat Med. 2023 Mar 17;: PMID: 36759673.

Ahmad-Nielsen SA, Bruun Nielsen MF, Mortensen MB, Detlefsen S. Frequency of mismatch repair deficiency in pancreatic ductal adenocarcinoma. Pathol Res Pract. 2020 Jun;216(6):152985. doi: 10.1016/j.prp.2020.152985. Epub 2020 Apr 22. PMID: 32360245.

Stathis A, Moore MJ. Advanced pancreatic carcinoma: current treatment and future challenges. Nat Rev Clin Oncol. 2010 Mar;7(3):163-72. doi: 10.1038/nrclinonc.2009.236. Epub 2010 Jan 26. PMID: 20101258.

Stein TA, Bailey B, Burns GP. Hepatopancreatic uptake and elimination of 5-fluorouracil after intravenous injection. Surg Oncol. 1993;2(1):43-9. doi: 10.1016/0960-7404(93)90043-x. PMID: 8252192.

Tassone E, Muscolini M, van Montfoort N, Hiscott J. Oncolytic virotherapy for pancreatic ductal adenocarcinoma: A glimmer of hope after years of disappointment? Cytokine Growth Factor Rev. 2020 Dec;56:141-148. doi: 10.1016/j.cytogfr.2020.07.015. Epub 2020 Aug 8. PMID: 32859494.

Tolonen N, Doglio L, Schleich S, Krijnse Locker J. Vaccinia virus DNA replication occurs in endoplasmic reticulum-enclosed cytoplasmic mini-nuclei. Mol Biol Cell. 2001 Jul;12(7):2031-46. doi: 10.1091/mbc.12.7.2031. PMID: 11452001; PMCID: PMC55651.

Tsien RY. The green fluorescent protein. Annu Rev Biochem. 1998;67:509-44. doi: 10.1146/annurev.biochem.67.1.509. PMID: 9759496.
Vincent A, Herman J, Schulick R, Hruban RH, Goggins M. Pancreatic cancer. Lancet. 2011 Aug 13;378(9791):607-20. doi: 10.1016/S0140-6736(10)62307-0. Epub 2011 May 26. PMID: 21620466; PMCID: PMC3062508.

Vogelstein B, Kinzler KW. Cancer genes and the pathways they control. Nat Med. 2004 Aug;10(8):789-99. doi: 10.1038/nm1087. PMID: 15286780.

Von Hoff DD, Ervin T, Arena FP, Chiorean EG, Infante J, Moore M, Seay T, Tjulandin SA, Ma WW, Saleh MN, Harris M, Reni M, Dowden S, Laheru D, Bahary N, Ramanathan RK, Tabernero J, Hidalgo M, Goldstein D, Van Cutsem E, Wei X, Iglesias J, Renschler MF. Increased survival in pancreatic cancer with nab-paclitaxel plus gemcitabine. N Engl J Med. 2013 Oct 31;369(18):1691-703. doi: 10.1056/NEJMoa1304369. Epub 2013 Oct 16. PMID: 24131140; PMCID: PMC4631139.

Waddell N, Pajic M, Patch AM, Chang DK, Kassahn KS, Bailey P, Johns AL, Miller D, Nones K, Quek K, Quinn MC, Robertson AJ, Fadlullah MZ, Bruxner TJ, Christ AN, Harliwong I, Idrisoglu S, Manning S, Nourse C, Nourbakhsh E, Wani S, Wilson PJ, Markham E, Cloonan N, Anderson MJ, Fink JL, Holmes O, Kazakoff SH, Leonard C, Newell F, Poudel B, Song S, Taylor D, Waddell N, Wood S, Xu Q, Wu J, Pinese M, Cowley MJ, Lee HC, Jones MD, Nagrial AM, Humphris J, Chantrill LA, Chin V, Steinmann AM, Mawson A, Humphrey ES, Colvin EK, Chou A, Scarlett CJ, Pinho AV, Giry-Laterriere M, Rooman I, Samra JS, Kench JG, Pettitt JA, Merrett ND, Toon C, Epari K, Nguyen NQ, Barbour A, Zeps N, Jamieson NB, Graham JS, Niclou SP, Bjerkvig R, Grützmann R, Aust D, Hruban RH, Maitra A, Iacobuzio-Donahue CA, Wolfgang CL, Morgan RA, Lawlor RT, Corbo V, Bassi C, Falconi M, Zamboni G, Tortora G, Tempero MA; Australian Pancreatic Cancer Genome Initiative, Gill AJ, Eshleman JR, Pilarsky C, Scarpa A, Musgrove EA, Pearson JV, Biankin AV, Grimmond SM. Whole genomes redefine the mutational landscape of pancreatic cancer. Nature. 2015 Feb 26;518(7540):495-501. doi: 10.1038/nature14169. PMID: 25719666; PMCID: PMC4523082.

Wilkinson L. Jenner's smallpox vaccine. The riddle of vaccinia virus and its origin. Med Hist. 1982 Jan;26(1):94–5. PMCID: PMC1139117.

Woo Y, Zhang Z, Yang A, Chaurasiya S, Park AK, Lu J, Kim SI, Warner SG, Von Hoff D, Fong Y. Novel Chimeric Immuno-Oncolytic Virus CF33-hNIS-antiPDL1 for the Treatment of Pancreatic Cancer. J Am Coll Surg. 2020 Apr;230(4):709-717. doi: 10.1016/j.jamcollsurg.2019.12.027. Epub 2020 Feb 4. PMID: 32032721.

Yanagi Y, Takeda M, Ohno S. Measles virus: cellular receptors, tropism and pathogenesis. J Gen Virol. 2006 Oct;87(Pt 10):2767-2779. doi: 10.1099/vir.0.82221-0. PMID: 16963735.

Yurttas C, Berchtold S, Malek NP, Bitzer M, Lauer UM. Pulsed versus continuous application of the prodrug 5-fluorocytosine to enhance the oncolytic effectiveness of a measles vaccine virus armed with a suicide gene. Hum Gene Ther Clin Dev. 2014 Jun;25(2):85-96. doi: 10.1089/humc.2013.127. PMID: 24933569.

Xia X, Wu W, Huang C, Cen G, Jiang T, Cao J, Huang K, Qiu Z. SMAD4 and its role in pancreatic cancer. Tumour Biol. 2015 Jan;36(1):111-9. doi: 10.1007/s13277-014-2883-z. Epub 2014 Dec 3. PMID: 25464861.

Zamarin D, Holmgaard RB, Subudhi SK, Park JS, Mansour M, Palese P, Merghoub T, Wolchok JD, Allison JP. Localized oncolytic virotherapy overcomes systemic tumor resistance to immune checkpoint blockade immunotherapy. Sci Transl Med. 2014 Mar 5;6(226):226ra32. doi: 10.1126/scitranslmed.3008095. PMID: 24598590; PMCID: PMC4106918.

**ACKNOWLEDGEMENT**

Mein Dank geht vor allem zunächst an meinen Doktorvater Herrn Prof. Ulrich M. Lauer für die Konzeption der Forschungsarbeit, die hervorragende Betreuung, die sowohl inhaltliche, als auch moralische Unterstützung, sowie die unglaubliche Geduld bei der Verfassung dieser Dissertationsschrift.

In gleichem Maße geht mein Dank an meine Betreuerin Frau Dr. Susanne Berchtold, die mir ebenfalls jederzeit mit Wissen, Rat und Hilfsbereitschaft zur Seite stand. Des Weiteren geht mein Dank auch an alle Mitarbeiter der AG Lauer / Bitzer mit Prof. Michael Bitzer, Irina Smirnow, Andrea Schenck, Christine Geißler, Dr. Julia Beil, Dr. Martina Zimmermann, Prof. Sascha Venturelli, Christian Leischner und Dr. Alexander Berger.
Nicht unerwähnt lassen möchte ich ebenso meine „ehemaligen“ Mitdoktoranden Nora Mayer, Markus Noll, Verena May, Can Yurttas, Christian Raff, Christer Ruff und Severin Schricker.
Ein besonderer Dank geht an meinen guten Freund Stavros Sotiriadis, der mich bei der Fertigstellung dieser Dissertation besonders unterstützt hat.

Zu guter Letzt geht man Dank natürlich noch an die Personen, ohne deren Beistand diese Dissertation niemals möglich gewesen wäre: meine Ehefrau Jessica, sowie meine Kinder Matilda, Greta und Lilia Klein.